Author:
Conole, Eleanor L S

Title:
Postnatal development of the mouse barrel cortex

investigating the intrinsic properties of spiny stellate neurons across the first two weeks of life

Postnatal development of the mouse barrel cortex:

investigating the intrinsic properties of spiny stellate neurons across the first two weeks of life

Eleanor Lucy Shepherd Conole

Department of Biomedical Sciences
UNIVERSITY OF BRISTOL

A dissertation submitted to the University of Bristol in accordance with the requirements of the degree of MASTERS BY RESEARCH in the Faculty of Life Sciences.

Word count: nineteen thousand eight hundred

May 2019

This thesis is dedicated to Alex Elsmore who died tragically by suicide in 2018. I am indebted to Alex for being such a great flatmate during my time at Bristol and for our many conversations about music, literature and science. Alex was awarded First Class in his MEng (Hons) degree in Electrical Engineering in July 2018, posthumously. I would like to use this opportunity to raise awareness for the risk of suicide in academic institutions and to promote a greater level of understanding, access to resources and support for students at vulnerable stages in their careers.

Declaration

I declare that the work in this dissertation was carried out in accordance with the requirements of the University's Regulations and Code of Practice for Research Degree Programmes and that it has not been submitted for any other academic award. Except where indicated by specific reference in the text, the work is the candidate's own work. Work done in collaboration with, or with the assistance of, others, is indicated as such. Any views expressed in the dissertation are those of the author.

SIGNED: ..... DATE: .....

Eleanor Lucy Shepherd Conole
May 2019

Acknowledgements

I am forever grateful to my supervisor, Dr Mike Ashby, for his advice, help and support over the entire duration of this Masters. His patience and understanding during every stage of this project (from my first dissection to the writing of this thesis) has been completely invaluable. He also inspired me to pursue a PhD: a conversation during my final year BSc research project about the chance to work on a question that is entirely yours has always stuck with me and still motivates me today. I would also like to thank every member of the Ashby lab who encouraged me to apply for to the Wellcome Trust Translational Neuroscience PhD programme in Edinburgh. The atmosphere of the Ashby lab, quality of research and conversations within it made me realise how lucky I am to be starting a career in science. In Bristol I was surrounded by people who encouraged curiosity and persistence and who also made my day-to-day research feel exciting and important.

For getting to grips with electrophysiology I owe thanks to Matt Udakis, Travis Bacon and Jon Witton for being an endless source of support when my rig acted up and for managing not to laugh when I turned up at their desks looking pained and unnecessarily distressed. I also owe a lot of hours in trying to understand MATLAB to Rob Lees who displayed amazing patience during my despairing-stage of learning to code (yet equal lack of awareness in portion sizes when compiling the shopping list for the lab-retreat; 4 carrots between 11 people!) and to Dani Franchini for first showing me how to patch a cell and for making me laugh lots since. Special appreciation and recognition goes to Fliss Inkpen, who set the groundwork for this investigation into postnatal development and for her encouragement and support when I needed it most.

Finally, thanks to the people in my life who lived with me while I was writing this and are no doubt just as relieved that I have finally finished: in Bristol, Tabby Conole and Elodie Cox and in Edinburgh, Rosalyn Pearson and Fred Tomlinson. Thank you for putting up with me.

Abstract

Sensation and perception are key aspects of cognition and healthy adult brain functioning. A region of the brain called the somatosensory cortex is responsible for the integration of sensory information. At the level of cortical circuits, key developmental time windows have been identified where significant changes in plasticity, synaptogenesis and spontaneous activity occur. It appears that disturbances to these processes can result in global impacts on cognition and behaviour, potentially underlying various neurodevelopmental disorders. A starting point to unpicking this complexity is to decode the biophysical changes that occur to healthy neurons during development. This report presents whole cell current clamp electrophysiology data obtained from layer IV spiny stellate neurons in the mouse barrel cortex over the first 2 weeks of life (postnatal days 4 - 14), focusing on changes to intrinsic properties with age, internal solution and temperature. Developmental changes were found in both the passive and active dynamics, with cells displaying decreased input resistance, increased action potential height, increased rate of rise and fall and decreased action potential width with age. A novel finding of this report is that intracellular infusion of biocytin induced development-dependent, temperature-independent changes in the active and passive dynamics of cells. These findings highlight the necessity for fine-tuning of concentrations of dyes when performing intracellular recordings, while widespread changes in the neuronal dynamics with altered temperature indicate the importance for standardised conditions in electrophysiology experiments. The observations in this report highlight how maturation of intrinsic properties is a complex, non-linear process that is prone to perturbation by external factors. These changes are likely due to developmental alterations in neuronal size, morphology, ion channel expression and activation and may reflect an overall increase in excitability and temporal precision of spiny stellate cells as they mature, allowing for more refined neural representation of sensory stimuli.

Word count: 299

Table of contents

List of figures

List of tables

Abbreviations

Greek Symbols

Ω	Ohm
τ_m	membrane time constant

Other Symbols

C_m	membrane capacitance
R_i	input resistance
R_m	membrane resistance

Acronyms / Abbreviations

aCSF	artificial cerebrospinal fluid
AIS	axon initial segment
AMPA	2-amino-3-(5-methyl-3-oxo-1,2- oxazol-4-yl) propanoic acid
ANOVA	analysis of variance
AP	action potential
ATP	adenosine triphosphate
CNS	central nervous system
CP	cortical plate
*DISC*1	disrupted-in-schizophrenia 1
DNA	deoxyribonucleic acid

*DTNBP*1 dystrobrevin binding protein 1

E embryonic day

EGTA ethylene glycol-bis(2-aminoethylether)-N,N,N',N'-tetraacetic acid

*FMR*1 fragile X mental retardation 1

GABA γ-aminobutyric acid

HEPES 4-(2-Hydroxyethyl)piperazine-1-ethanesulfonic acid

HRP horseradish peroxidase

KGlu potassium gluconate

KMeth potassium methylsulphate

KO knock-out

LTP long-term potentiation

MZ marginal zone

NMDA N-methyl-D-aspartate

*NRG*1 neuregulin 1

P postnatal day

PBS phosphate buffered saline

RMP resting membrane potential

SEM standard error of the mean

SS spiny stellate

SVZ subventricular zone

TC thalamocortical

VIC voltage gated ion channel

VPm ventroposteriormedial nucleus

VZ ventricular zone

WM white matter

WT wild type

Chapter 1

Introduction

1.1 General introduction

The ability of any organism to perceive and understand the world has to be rapid in order for them to survive. In mammals, the cerebral cortex has evolved to meet this demand, as a highly laminated structure capable of complex high-order sensorimotor function. Across the brain, the cortex is organised both horizontally into six distinct layers and vertically oriented columns (Lübke and Feldmeyer, 2007).

Sensation is in part controlled by an area of the cerebral cortex called the primary somatosensory cortex. In humans, this structure integrates external stimuli such as touch, sound, pressure, temperature, and pain to create a 'sensory homunculus': a sort of brain blueprint with neuronal representation of the anatomical regions of the human body. In rodents, this region of the brain has a specific division called the barrel cortex, where a similar somatotopy prevails – here the cytoarchiecture of the brain reflects the pattern of the whisker pad on the rodent's snout.

This somatotopic pathway is both well-defined and easily manipulated experimentally (via genetic, behavioural and molecular intervention) and has spurred a wealth of research into cortical plasticity and development (Ashby and Isaac, 2011; Crair and Malenka, 1995; Shimogori and Grove, 2001). There is clear importance of early postnatal sensory experience on network formation, with early sensory disruption such as whisker trimming having long term, irreversible effects on circuit formation in the mature cortex (Fox, 1992; Keller and Carlson, 1999). These impairments in circuit formation can have profound impacts on cognitive function in adulthood, with increasing links to developmental sensory perturbation and conditions such as schizophrenia (Stefansson et al., 2002) autism (Kroon et al., 2013; LeBlanc and Fagiolini, 2011; Wang et al., 2014) and various other neuro-developmental conditions (Harlow et al., 2010; Meredith et al., 2012). A greater understanding the biophysi-

cal changes occurring to individual neurons during healthy cortical development may aid understanding of mature mechanisms of sensory integration in pathophysiological states.

Across the first two postnatal weeks, neurons within the barrel cortex display huge changes in synaptogenesis (Ashby and Isaac, 2011), synaptic plasticity (Hardingham et al., 2003) and gene expression (Fox, 1992; Keller & Carlson, 1999). This is a period of synaptic refinement – where sensory information is beginning to be received and stored by the immature cortex – and the overall aim of this thesis is to investigate the maturation of neurons embedded within cortical networks.

The spiny stellate (SS) neuron is located within the fourth layer of the somatosensory cortex, forming recurrent connections with cells within the same barrels (Schubert et al., 2003). Earlier studies (Feldman et al., 1999; Holtmaat et al., 2006; Feldmeyer et al., 2013; Fox and Wong, 2005) have highlighted this neuronal subtype's importance in regulating cortical network changes in by performing experiments on the effect of experience (sensory stimuli) on early network formation, with layer IV being the earliest identified site of thalamocortical plasticity (Yu et al., 2012).

Several features of the SS neuron make it a good target for investigating plasticity in development. The combination of the spiny stellate neuron's specific location (confined to layer IV barrels), network importance (critical input layer for the cortex) and early developmental progression (other neurons within the barrel cortex, such as layer V pyramidal neurons, migrate through the layers at a later stage) make it an excellent starting point for this investigation.

This thesis is a tale of three separate investigations, each linked to how the barrel cortex develops in the first two weeks of life. The first focuses on the maturation of intrinsic properties of spiny stellate neurons from P4-P14. During the first two weeks of life, neocortical circuitry undergoes widespread reorganisation (McCormick et al., 1985) resulting in the refinement of spontaneous activity, transitioning from highly synchronised, oscillatory firing patterns (Khazipov and Luhmann, 2006; Yuste et al., 1995) to desynchronised firing patterns. The overall result of this is that the network tends towards a more efficient neural code (Golowasch et al., 2009). This transition is related to the intrinsic properties of neurons within such networks (Valiullina et al., 2016), and the developmental changes that they undergo, hence studying the intrinsic properties across the first 2 weeks of life in spiny stellate cells could give us a better understanding of overall cortical network development.

The second part of this investigation investigates the impact of distinct internal solutions on intrinsic properties. The practice of combining patch-clamping with protein or dye identification in the same cell is popular amongst neurophysiologists to help define which class, location and developmental stage of the neurons being recorded are from, and to

relate functional properties to cell morphology. However, there is a paucity of information regarding what the exact effects of these compounds are on neuronal electrophysiology. This work challenges the assumption that these compounds do not have divergent effects and aims to inspect the changes in basic electrophysiological properties in spiny stellate neurons when recorded using whole cell patch clamp using distinct internal solutions, focusing on the changes occurring during specific developmental age points from immature to mature networks.

The third and final aspect of this report focuses on how temperature affects intrinsic properties in development, with the aim of characterising both how temperature (room temperature vs 'physiological' temperature) affects active and dynamic properties of neurons across development and whether temperature has any differential effects on the pharmacology of the internal solutions.

1.2 Structural and functional development of the somatosensory cortex

1.2.1 The Protomap and Protocortex theories of development

Neurodevelopment is a complex interplay of experience and genetics. In the 1980s there were two opposing theories of cerebral cortex development: the 'protomap' and 'protocortex' models formulated by Pasko Rakic and David O'Leary respectively (Rakic, 1988; O'Leary, 1989). Rakic argued that to decipher the development of the cortex, the role of genes should be better understood first, and that genetics were the driving force behind cortex development. The evidence to back up this claim came from early investigations into neural precursor cells (Rakic, 1974a). In the embryonic brain, different pools of progenitor cells give rise to different neurons, which migrate to specific areas in the cortex due to specific genetic patterning. This is the blueprint to the laminar organisation of the embryonic telencephalon (the prenatal structure in the brain that develops into the cerebral cortex) and implies that even before any sensory input, neurons are pre-programmed to belonging to different regions of the brain and have a high degree of cell-fate dependability based on where they originated from. In contrast, a year later another neuroscientist, O'Leary, proposed the 'blank state' hypothesis of neurodevelopment: that post-neurogenesis, considerable modifications take place that result in the emergence of neocortical areas, encoded by early extrinsic factors rather than predetermined genetic cues. In the 30 years that have succeeded these theories, it seems that both contain some element of truth, with both early patterning of cortical lamination delineated by a genetic 'blueprint' and early sensory input shaping the formation

and clustering of neurons within cortical layers (Bystron et al., 2008; Kingsbury and Finlay, 2001; Ruiz et al., 2001). The development of the cerebral cortex is a multifaceted process shaped by the both the combination and the interaction of genetics, epigenetics, and both spontaneous and experience-dependent activity.

1.2.2 Inside out maturation of the somatosensory cortex

Instead of forming layer by layer, the laminar-organisation of the cortex develops in an inside-out fashion, with early brain cells (glia, neurons, astrocytes) residing in deep cortical layers and brain cells born at later stages populating the more superficial layers, as found out by early autoradiography investigations into cortex development and cell migration (Ruiz et al., 2001). Neurons are not static in development, and instead of originating in their final laminar-location, neurons migrate through the cortex as it develops (see figure 1.1: inside out maturation of the cortex) with the cortical plate giving rise to the different cortical layers.

Before birth, at E11, no 'cortical layers' as we know them have formed (Noctor et al., 2004). Instead, the preplate (PP), ventricular zone (VZ) and sub-ventricular zone (SVZ) appear, with the latter two regions containing pools of progenitor cells that later become various excitatory neurons and inhibitory interneurons (Hoerder-Suabedissen and Molnár, 2015). The PP gives rise to the subplate (SP) which eventually gives rise to the distinctive cortical columns, the migration of axons through cortical layers, and the maturation of excitatory and inhibitory circuitry (Kanold, 2009). Indeed, ablation experiments demonstrated that elimination of SP neurons profoundly alters cortex circuit maturation, with SP ablation after E15 preventing the strengthening of thalamocortical synapses in adult circuits, illustrating the key role that SP neurons play in circuit development. Neurons then travel via radial glia (Rakic, 1974b) from the SP to give rise to another two regions: the cortical plate (CP) and marginal zone (MZ) at around E15. At E18, thalamocortical afferents move through the cortical layers, with layer VI being formed first. Figure 1.1 depicts this process.

At birth (P0) layer IV and V are formed and thalamocortical afferents begin to project and innervate layer IV, initiating the formation of characteristic barrel cortex cortical columns (Fox, 2008). The neocortical architecture is considered complete by around P7: 'barrel' structures are clearly visible, most cell migration and proliferation has ended and thalamocortical afferents originating from the thalamus start to form synaptic connections in layer IV, giving rise to a richly interconnected cortical network that relays sensory processing.

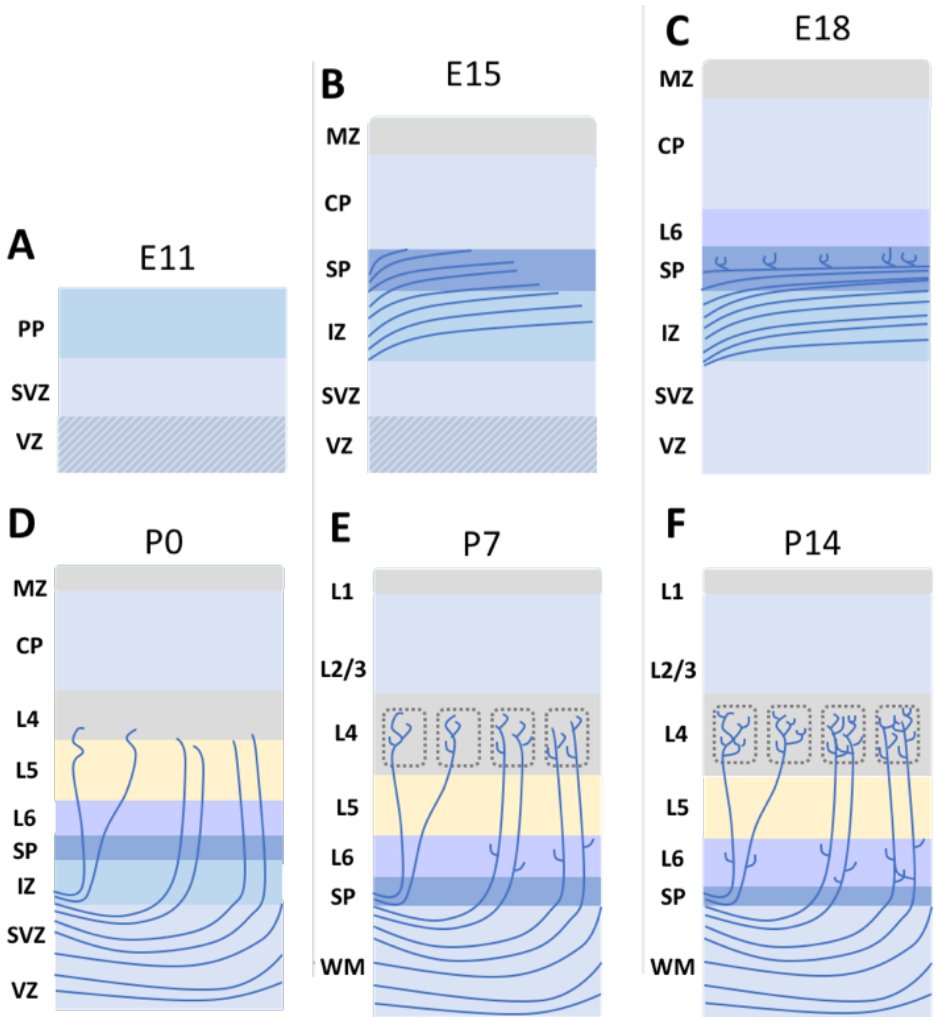

Fig. 1.1 **Inside out maturation of the cortex:**
Schematic depicting thalamocortical axon growth and development of the 6 distinct layers in the neocortex (A) At E11 the formation of the pre-plate (PP), the ventricular zone (VZ) and subventricular has occurred. The SVZ and VZ have distinct pools of progenitor cells that give rise to different neurons; together these zones eventually become the white matter (WM) of the neocortex (B) E15, thalamocortical axons project into the intermediate zone (IZ) (C) E18, thalamocortical axons form synapses with SP cells. (D) P0: Thalamocortical axons have formed synapses with SP cells and layer VI is formed. (E) P7: The 6 distinct strata of the cortex are visible, and the SP layer shrinks as cell death occurs to a population of SP neurons. Thalamocortical axons reach layer IV (their final destination) and arborize; immature circuits form between the SP and LIV. (F) By P16, thalamocortical axons have formed reciprocal connections in layer VI and increased arborisation in layer IV has occurred. There is a distinct 'clustering' of thalamocortical axons within the barrels. Adapted and modified from (Hoerder-Suabedissen and Molnar, 2015; Pinon et al., 2009)

1.2.3 Development of the barrel cortex

Distinctive 'barrels' (groups of neurons) visible in the fourth layer (IV) of the rodent somatosensory cortex give the barrel cortex its title. Discovered by scientists Woosley and Van der Loos in the 1970s, these structures led to increased understanding of the effect of experience and cortical processing in development.

Woosley and Van der Loos demonstrated the role of barrels as individual processing

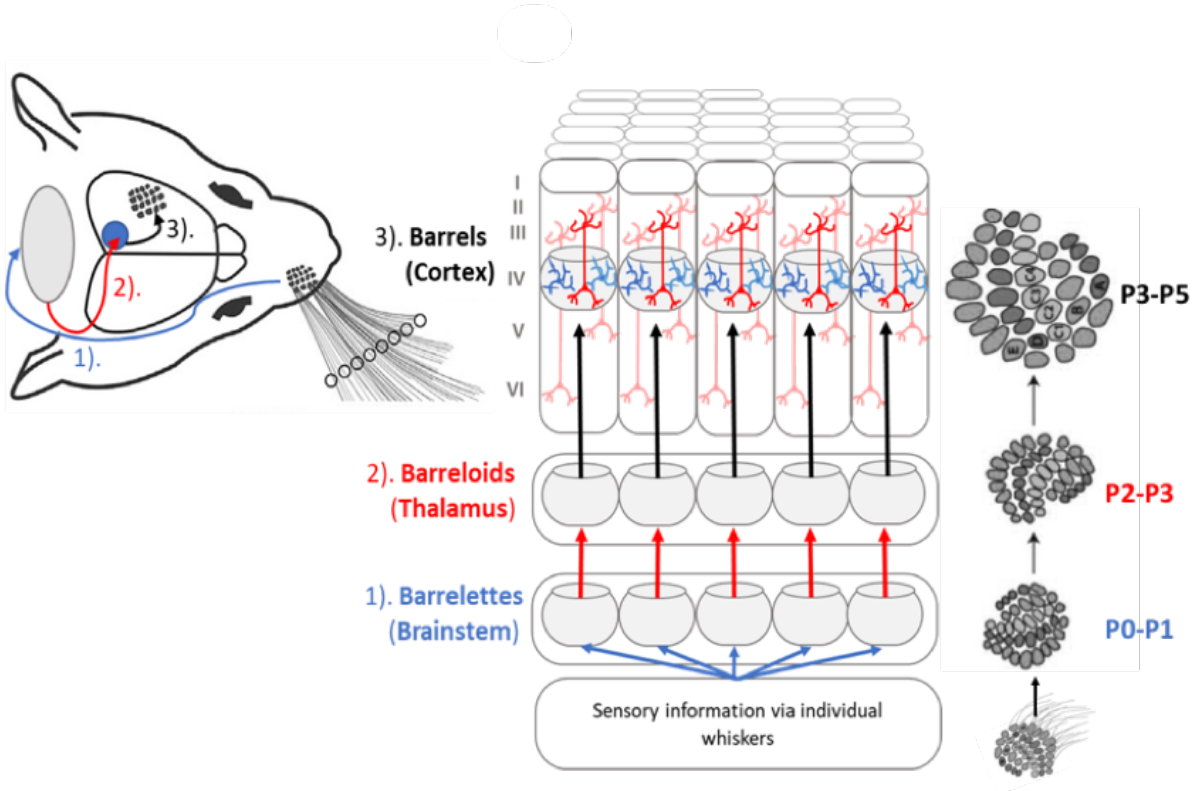

Fig. 1.2 **Whisker input pathway and somatotopy of the barrel cortex.**
Schematic demonstrating preservation of somatotopy, its development, and how sensory information from the whiskers on the mouse's nose travels to the 'barrel' structures in the PrV of the brainstem (barrelettes), to similar copies in the VPm of the thalamus (barreloids); then thalamocortical axons transfer input to barrels the barrel cortex, where spiny stellate (marked in blue; pyramidal neurons in red) neurons reside.

units that another scientist, Mountcastle, had identified in his investigations into cortical columns of cats a few years earlier (Woolsey and Van der Loos, 1970; Mountcastle, 1957). This characteristic patterning is replicated throughout the whisker-barrel pathway: from the mystacial vibrissae, to brainstem 'barrelettes', to barrreloids in the thalamus to the

eponymous 'barrels' of the cortex (Erzurumlu and Gaspar, 2012; Petersen, 2007; Sehara and Kawasaki, 2011). Figure 1.2 illustrates this system and illustrates how the development of this distinctive patterning of happens at different stages in development:

- Before birth, spontaneous activity instigiates the movement of neurons through the cortex
- By P0, projections to the thalamus have been established (Erzurumlu & Gaspar, 2012) and barrelettes are found in the brainstem (Van Der Loos, 1976)
- Barreloids, by contrast, occur around P2-P3 in a region of the thalamus called the the ventro-posterior-medial nucleus (VPm) (Durham and Woolsey, 1984)
- The distinctive 'barrels' themselves form around P3-P5 (Van Der Loos & Woolsey, 1973)

This somatotopic conservation was discovered by sensory-deprivation experiments (Van Der Loos, 1976; Durham and Woolsey, 1984), paving the way for investigating the how experience-dependent plasticity shapes the formation of the somatosensory cortex in development.

1.2.4 Diversity and development of excitatory neurons in the barrel cortex

Within the barrel cortex, two main types of neurons exist: excitatory and inhibitory neurons. The main distinction between these cell types is that excitatory neurons transmit information to one another via the neurotransmitter glutamate whereas inhibitory neurons use gamma-aminobutyric acid (GABA) (Petersen, 2007). Interneurons are a more heterogenous group, displaying huge diversity in the roles and proposed number of different subtypes (Markram et al., 2004), excitatory cells, by contrast, constitute a much more uniform group consisting of 3 key subtypes: pyramidal and star pyramidal and spiny stellate cells, though within these subtypes there is further diversity as outlined in figure 1.3. Within the barrel cortex, excitatory neurons greatly outnumber interneurons (Sun et al., 2006), though both excitatory and inhibitory networks interact together in order to shape information processing from the thalamus ascending to the cortex (Petersen, 2007).

Spiny stellate (SS) neurons ('stellate' due to their star-shaped-appearance and 'spiny' owing to the number of spines on their dendrites) are the focus of this investigation. Their characteristic morphology and location (within Layer IV barrels) makes them a reliable target

for whole cell electrophysiology experiments, given that barrels can be visually distinguished in the slice and stellate cells can be easily identified with the distinct spherical morphology of their soma. Functionally, spiny stellate neurons have critical task in the integration of sensory inputs. They form a highly interconnected local excitatory network and are specialised in receiving and amplifying information from thalamic synapses, acting as an important relay in sensory information from the rodent's whiskers. Excitatory circuitry between SS cells is functionally confined to individual barrels, as determined by paired-recordings (Petersen & Sakmann, 2000) performed in barrel cortex; a discovery that led to the theory that individual barrels in the barrel cortex act as functionally independent processing columns (Petersen & Sakmann, 2001).

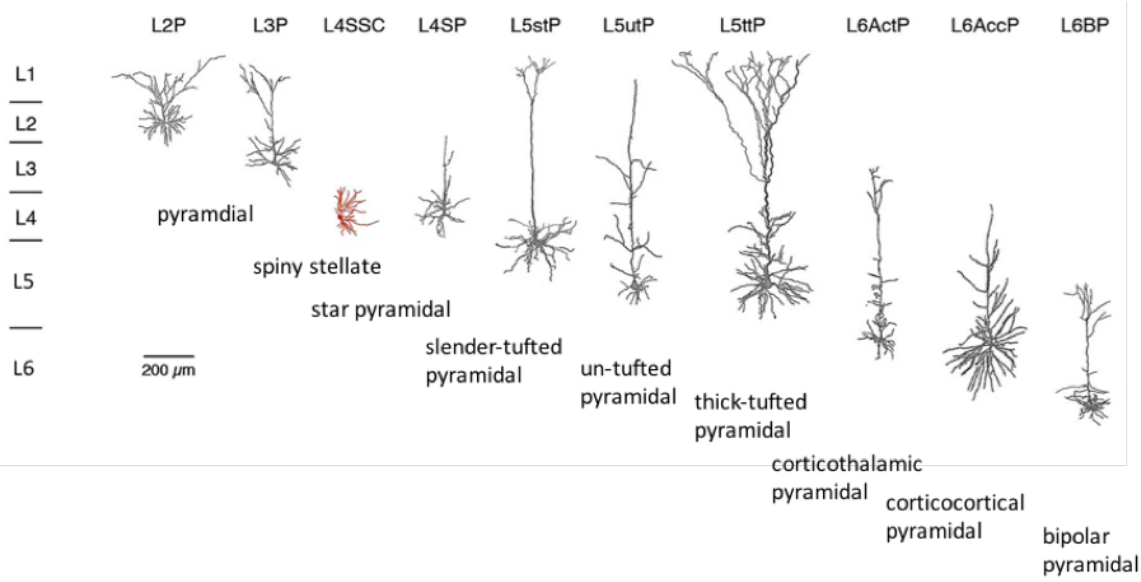

Fig. 1.3 **Morphological differences of excitatory neurons in the somatosensory cortex:** 10 different excitatory neuron types, Layer IV spiny stellate neuron coloured in red for clarity. There is an incredible range of morphological diversity in the dendritic branching and apical dendrite length of most excitatory neurons; spiny stellate neurons lack the distinctive apical dendrite of pyramidal cells. Adapted from (Radnikow and Feldmeyer, 2018)

The developmental progression of spiny stellate cells also makes them an interesting target of study. As outlined previously, all neurons start off similar in the progenitor cell pools, which change in morphology through development due to a mix of extrinsic and intrinsic cues, before residing in their final location in one of the distinct cortical layers (see figure 1.1). Callaway and Borrell (2011) used *in utero* electroporation of DNA to progenitors

located in the CP zone of the neocortex to decode the morphological progression of neurons within layer IV, shedding insight into spiny stellate neuron maturation.

At P0, spiny stellate neurons have round soma and thick apical dendrites – they are distinct from other excitatory neurons (such as pyramidal neurons) which are migrating through the cortical layers, as these cells have more oval-shaped soma and markedly thinner processes (see figure 1.3). From P0-P3, spiny stellate neurons, regardless of where they are within a barrel, orient their dendrites towards the centre, where thalamocortical axon termini reside. 2-photon imaging revealed that NMDARs regulate the dynamics of this process and have an impact on the dendrite orientation of SS neurons, as in NMDAR-deficient neurons there are greater degrees of dendrite motility and less specific orientation (Mizuno et al., 2014). Stellate cells become visually distinctive and characteristic in morphology (with round soma, and 'star'-like projections) from P5 and are considered morphologically mature by P10, with both their axon and dendrites directed towards the centre of the barrel (Callaway and Borrell, 2011). Investigating the biophysics of these neurons during the first two postnatal weeks is of interest considering the dynamic changes happening to the morphology of these cells during this period.

While the development of spiny stellate cells and therefore excitatory neurotransmission is focused on in this thesis, it is important to credit the importance of inhibitory synapses in development. GABAergic circuitry in the somatosensory cortex is made up of great range of classes of inhibitory neurons and the developmental trajectory of these cells has been under considerable investigation (Miyoshi et al., 2007; Butt et al., 2005). Worthy of note here is the role of inhibitory currents early in development; Ben-Ari (2002) found that instead of inhibiting early excitation as they would in adulthood, postnatal GABAergic synapses actually facilitate it – this is due to an increase in the Cl^- reversal potential in nascent synapses, resulting in $GABA_R$ activation causing depolarisation. As the development of excitatory circuits occurs before inhibitory networks, early excitatory dominance means that excitatory pathways such as those established between SS neurons can strengthen before any influence of inhibitory inputs.

1.2.5 Critical periods in development

Sensory systems display high susceptibility to perturbations of input in a key developmental time period, resulting in morphological and functional changes in the cortex. The term 'critical period' was coined to describe this window: the formation of neocortical circuitry relies upon sensory-experience (Hensch, 2005) and disruption during formation can result in permanent changes in mature circuits. The seminal studies on critical period plasticity were performed in the 1960's by Hubel and Wiesel, who devised sensory deprivation paradigms

for kittens, demonstrating how deprivation of sensory input during a key developmental window resulted in impaired formation of visual processing pathways (Hubel and Wiesel, 1963). These experiments were adopted and modified by Van Der Loos and Woolsey in the 1970s, who showed that there were critical periods in somatosensory system as well: whisker-trimming experiments revealed that early developmental deprivation of stimuli causes impaired cortical formation of the barrel cortex. Since these early breakthroughs in the field, a large number and range of critical periods have been defined across the brain (de Villers-Sidani et al. 2007; Stern et al., 2001; Wen and Barth, 2011). Critical periods have large implications for neurodevelopmental disorders (Brandon et al., 2004; LeBlanc and Fagiolini, 2011; Wang et al., 2014) and investigating these key age points could help us better understand how these connectivity motifs are formed and how this early susceptibility to circuit disruption can cause lasting changes in adult information processing and cognition. They are relevant to this study, as in the barrel cortex, distinct critical periods occur during these postnatal weeks:

- **P0-P4:** A 'structural' critical period where the mapping of thalamocortical (TC) afferents to layer IV is refined. Electrophysiology studies *in vitro* show that this is the critical period for LTP (a form of synaptic plasticity) at thalamocortical silent synapses (Crair and Malenka, 1995) and studies *in vivo* by Fox (1992) outlined – through whisker-deprivation experiments in the rat – how this is a key period for the topographic arrangement of whisker fields; if sensory experience is perturbed during this time, the characteristic patterning of somatotopic barrels do not form properly (Fox, 1992).

- **P4-P7:** The maturation of TC synapses results in modification of glutamate receptors, with the number of AMPA receptors (AMPAR) increasing disproportionately to NMDA receptors (NMDAR) (Crair and Malenka, 1995). Moreover, the amount of NMDAR-containing without AMPAR synapses (so called 'silent' synapses) are rapidly reduced (Ashby and Isaac, 2011; Isaac et al., 1997). Daw et al., (2006) depicted that the biophysical differences between these two glutamate receptor types underpins the maturation of sensory signalling in cortical circuits, finding telltale changes in their deactivation kinetics and their excitatory postsynaptic potentials (Daw et al., 2006)

- **P10-P14:** layer four to layer three synapses have a CP between P10-14 (Lendvai et al., 2000; Stern et al., 2001); 2-photon experiments revealed that sensory experience drives structural plasticity in dendrites during P11-P13, with whisker-trimming degrading the tuning of layer II/III receptive fields (Lendvai et al., 2000).

1.3 Why investigate intrinsic properties of neurons?

Whole-cell patch-clamping is a traditional method used in neuroscience research to investigate the electrical properties of neurons. This method provides an efficient measurement of both passive and active properties and offers complete access and control of the cell at relatively low cost. During the first two postnatal weeks, neurons undergo drastic transformations in their morphology and connectivity (Ashby and Isaac, 2011.; Suter et al., 2013; Valiullina et al., 2016) and exhibit changes in the insertion, activation, inactivation, density, type and subunit composition of ion channels within their membranes. One way to study these changes in an isolated system is to look at the intrinsic properties of individual neurons: their active and passive dynamics.

1.3.1 Passive dynamics

Passive dynamics describe the passive membrane properties of neurons; they influence how efficient synapses are and determine the rate at which voltage can move along parts of the neuron. There are distinct passive properties of neuronal membranes that influence their electrical activity that can be readily investigated via electrophysiology and include the resting membrane potential, membrane time constant, capacitance, and input resistance; each of these will be described in turn.

1. **Resting membrane potential (RMP):** the RMP of neurons arises due to the distribution of ionic forces across the plasma membrane (see figure 1.4A below). The RMP plays a key role in neuronal functioning; there are diverse changes to the RMP over development (Ben-Ari, 2002; Moody & Bosma 2005; Crair & Malenka, 1995; McCormick et al., 1985). At young developmental time points, there are less sodium (Na^+) channels in the plasma membrane, causing the balance of ionic currents to be different in immature neurons to mature ones (Ben-Ari, 2000). As neurons mature, there is also increased conductance of potassium through potassium leak channels as well as an overall decrease in intracellular chloride ions (Ben-Ari, 2002). These various changes in the ionic properties of the cell influence the overall RMP; it will be interesting therefore to investigate how the RMP changes over the course of development and try to relate this to the underpinning biophysics (i.e. movement of ions).

2. **Membrane capacitance (C_m):** The cell membrane of neurons acts as a leaky capacitor: as lipid bilayer (around 8-10nm across), it acts both to insulate the cell and separate intracellular and extracellular contents, and charges and is a key indicator of the functioning of neurons (Rall et al., 1962; Cole, 1968; Jack et al., 1983); see figure

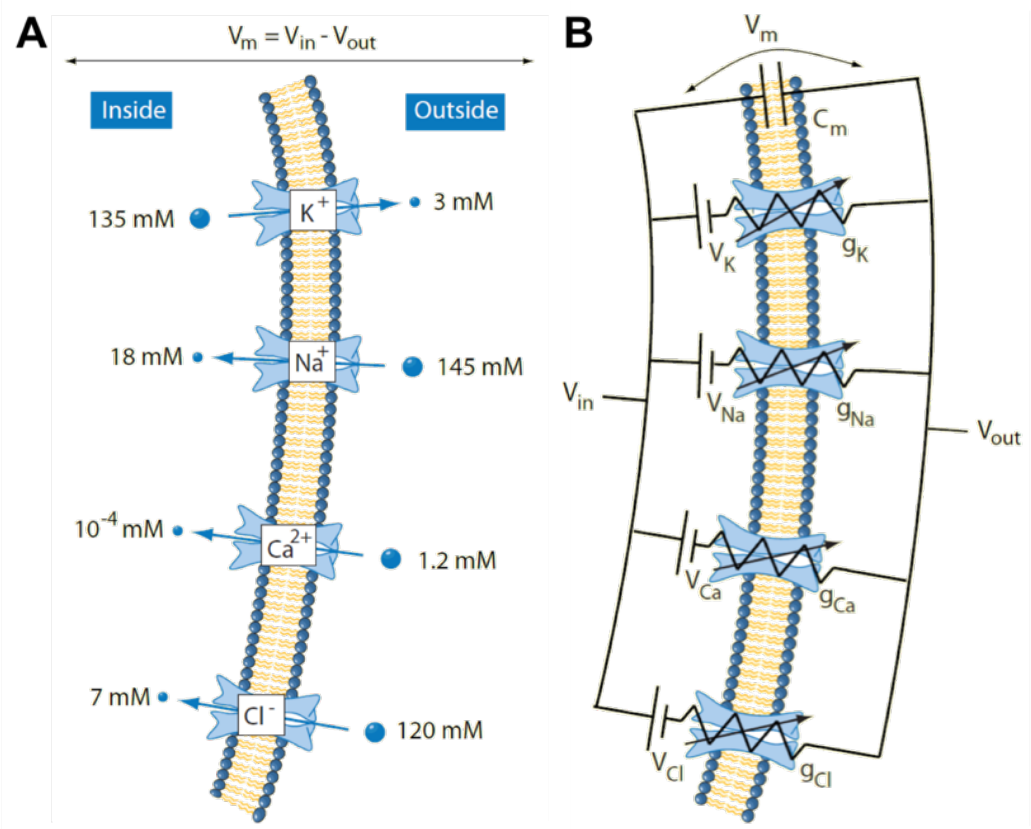

Fig. 1.4 **The RMP: differential distribution of ions across the cell membrane** (A) schematic displaying sodium, calcium, potassium and chloride ions and their concentrations; these ionic differences create ionic balances that give result in the RMP (B) Equivalent model circuit diagram of the plasma membrane; various passive membrane properties can be derived from modelling the plasma membrane as an electrical circuit, with individual ion channels understood as resistors (springs) with varying conductances associated with their ions (V_{ion}). The phospholipid bilayer can be modelled as a capictor, giving rise to cell capacitance (C_m). Adapted from (Bean, 2007)

1.4B. As there is an ionic concentration difference across the bilayer it stores energy in an electric field. The specific capacitance of cell membranes is determined by their lipid and protein constituents; C_m is referred to as a 'biological constant' (around 1.0 $\mu F/cm_2$) – as estimated by investigations into the giant squid axon (Curtis and Cole, 1938; Hodgkin and Huxley, 1952) and measured through whole-cell patch clamp investigations in mast cells (Solsona et al., 1998). However this is ignoring variation between cells; recent studies (Thurbon et al., 1998; Chitwood et al., 1999) suggest that not only is C_m not technically equivalent across neuronal populations, but it could also vary throughout the dendritic processes of a single neuron.

3. **The membrane time constant (τ_m)** describes the degree of change of voltage across the cell membrane and is defined as the cell's membrane resistance multipled by its capacitance ($\tau_m = C_m \times R_m$); in electrophysiology experiments, τ_m can be measured fitting an single exponential to the potential difference before the voltage has reached a steady state (i.e. whilst the membrane is charging). In this particular investigation cell capacitance was not estimated. However, if the biological constant approach is adopted, a larger neuron with a larger cell membrane will have greater capacitance; therefore, over the course of development the membrane time constant would be expected shorten from P4-P14.

4. **Input resistance (R_i)** determines the difficulty for current to cross the cell membrane of a neuron. As the membranes of neurons are lipid based, it is hard for ions to freely move either side of the plasma membrane, resulting in the membrane of neurons having a high resistance (Stein, 1986). Only very small, uncharged molecules (such as O_2, H_2O, CO_2) can diffuse freely through the membrane (Cooper, 2000). This is why ion channels are present within neuronal membranes; they allow ions to cross readily in and out of the membrane, lowering the resistance of the membrane (n.b. although there are also pump proteins in the cell membrane, ion channels only allow ions to move passively, i.e. they do this without ATP). Input resistance therefore reveals a lot about the physiological state of the cell at rest: its size, density of ion channels and proportion of ion channels open (Kandel et al., 2000).

1.3.2 Active dynamics

Action potentials (APs), characteristic hallmarks of neuronal communication and activity, are a classic starting point for investigating neural dynamics. APs are significant alterations in the membrane potential of neurons, characterised as sudden, sharp uprises of voltage; they are time-dependent, specific to brain-cells, and the language of synaptic connectivity.

APs' roles are varied and complex, from the direct influence of regulation of calcium (Ca^{2+}) channels (Simms and Zamponi, 2014), to the indirect result of influencing entire neuronal networks. The AP waveform is formed by various currents from both passive cell dynamics (those relating to the membrane potential of neurons) and active dynamics (ion channel dependent dynamics). As neurons develop, they grow and change shape: such changes are reflected in the composition and morphology of their membranes, and in turn the shape of the AP waveform. The AP can be broken down into distinct measurable components: its threshold, its height and its width; and the rate at which the upstroke of AP rises and falls.

The AP threshold is the level of depolarisation at which voltage-gated Na^+-channels in the cell membrane become unclosed, allowing sodium to flow in and depolarise the cell (Figure 1.5B). This process is resurgent: as Na^+ ions flow in the cell they depolarise it further thus causing more Na^+ channels to open (Figure 1.5B). APs can therefore propagate in this way as the axial membrane becomes depolarised – this process is illustrated in Figure 1.5 below. APs are described as operating by an 'all-or-nothing' law whereby an AP signal can only be generated if its AP threshold has been surpassed; the depolarisation afterwards will be consistent irrespective of the original size of the synaptic input (Bean, 2007).

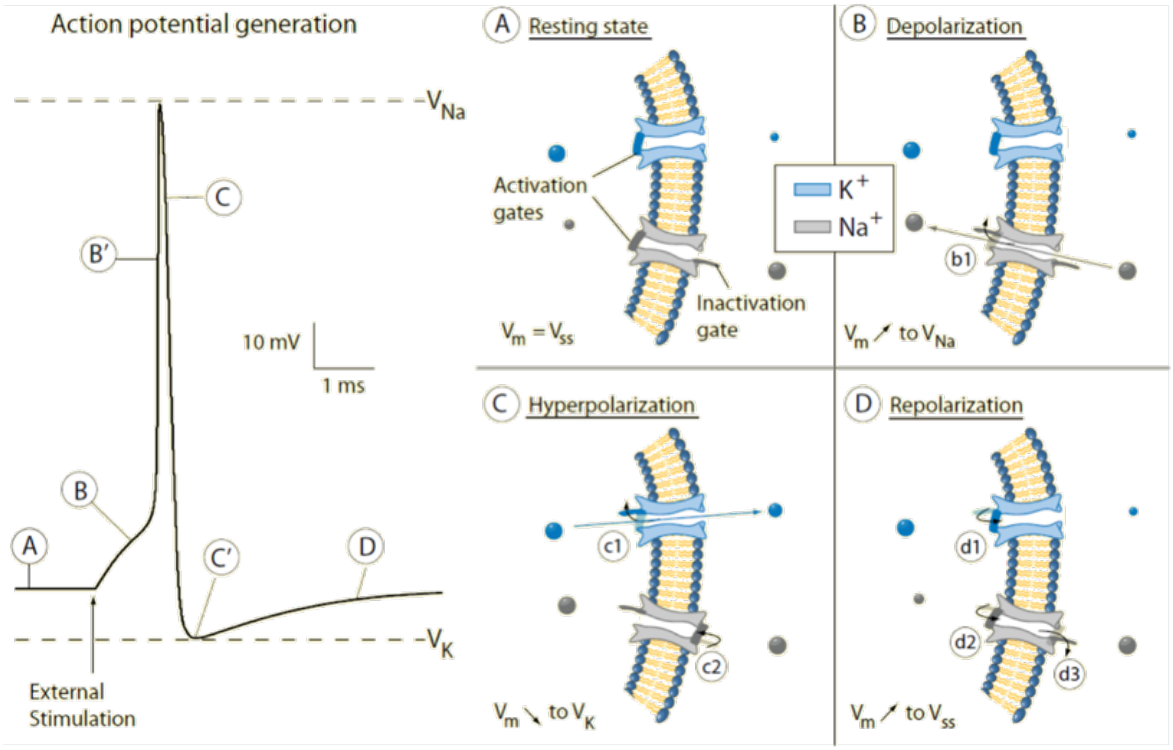

Fig. 1.5 **Mechanisms of action potential generation**
Schematic diagram of an action potential and how it propagates along a neuronal membrane. Left schematic displays AP segmented into various time points. (A-D) which are depicted on the right in terms of various fluxes of ions in and out of the neuronal cell membrane. These fluxes, caused by voltage gated ion channels (VICs) opening and closing, underlie the changing morphology of the AP. Adapted from (Bean, 2007)

While APs are 'all-or-nothing', a neuron must have a way to bring its electrical conductance back to normal – a sort of 'homeostasis' for its own activity. Such a mechanism lies in the form of voltage gated K^+ channels. These channels open with a slight delay (See Figure 1.5 C-D) and permit K+ to leave the cell, reversing the depolarisation caused

by the Na^+ influx. At the same time, another physiological mechanism is put in place to restore homeostasis: rapid inactivation of the voltage-gated Na+ channels. As the sodium channels inactivate (i.e. close), the membrane potential tends back to its resting state. Finally, there is the hyperpolarisation of the neuron (see figure 1.5C): after another delay, potassium channels close, causing the membrane potential to go past its resting state, making it 'hyper-polarised'. The ion concentrations then return, gradually, to their resting levels (Fig 1.5D: 'repolarisaiton') causing the cell to returns to its RMP of around 70mV.

These mechanisms mean that the AP depolarisation of the neuronal membrane is very brief, usually only around 1 – 2 ms (Bean, 2007). Although all APs are governed by the same ionic properties, and despite the ubiquitous nature of these homeostatic-mechanisms in neurons, the shape of an action potential is not uniform. Different neuronal subtypes have different neuronal shapes; neurons at different developmental time points vary in size and shape; and there is a vast array of types of VICs that are expressed by different neurons, in different quantities. Furthermore, voltage-gating of ion channels varies between different neurons and even within different regions of the same neuronal membranes. Bear (2007) illustrates this point with an example in the hippocampus: Na+ channels in mossy fibre synapses inactivate at 2x the speed of sodium channels in the soma of granule cells.

The intrinsic properties of SS neurons in layer IV of the barrel cortex have not been thoroughly investigated over P4-P14, and so patching these neurons across this time-window and relating them to the plasticity events emerging over this time could provide us with key insights in the cellular mechanisms of cortical circuit development.

1.4 Development of intrinsic properties

Early studies into development in the cerebral cortex (McCormick Prince 1987) found that action potentials of young neurons (P0-P7) had significantly longer widths and smaller peak amplitudes than those at later developmental time points (P17). This was accompanied by equivalent changes in the kinetics governing action potentials, with reduced rates of rise and fall in immature neurons. More recent studies since these early investigations indicate that developmental-dependent changes in the electrical neuronal properties occur across many cortical regions: in the somatosensory cortex, studies on layer II/III neurons (Maravall et al., 2004); in the visual cortex, layer V pyramidal neurons (Etherington & Williams, 2011; Kasper et al., 1994) and layer V pyramidal neurons (Zhang 2004) and SS neurons in layer IV (Valiullina et al., 2016). These investigations also add to the concept of critical periods in development (see section 1.2.5), with greater shifts in changes occurring during specific windows of development.

Neuronal cell fate is partially determined by genetics, as discussed previously in section 1.2.2, however since the intrinsic passive dynamics of cells are linked to cell morphology, factors such as neurotrophins, morphogens and various growth factors are also important (Pierani and Wassef, 2009). The age of cortical neurons affects the excitability properties of the different cortical layers and the subpopulations of neurons within the distinct layers means that there are functionally distinct roles across the cortex. The origin and timing of various neurons determines their physiology in mature cortex. For example, interneurons in the developing ventral telencephalon have a set developmental trajectory depending upon where they were first formed (Butt et al., 2005). In contrast to this pre-programmed effect, guidance signals and neurotrophic factors (Whitford et al., 2002) have been shown to affect the final topographical location and cellular differentiation of cortical neurons. Development of electrical proprieties of neurons therefore appears to be a contribution of both extrinsic and intrinsic factors.

1.5 The impact of different internal solutions on intrinsic properties

In order to effectively study neuronal dynamics *in vitro*, the experimental setup and recording environment must replicate the physiological conditions of a neuron as well as maintain this state over the course of an experiment. In whole-cell electrophysiology, the internal solution is a crucial and delicate component of the experiment, as subtle changes in ionic composition can impact the electrical properties of the neurons being patched (Kay, 1992).

Good internal solutions should emulate the intracellular environment of a neuron whilst allowing for electrophysiological investigations and potential staining and post-hoc recovery. However ionic-balances are not set: variation in neuron type and developmental age results in a heterogeneous distribution of ion channels. It is important to bear this in mind with electrophysiology experiments performed in this study – the cells patched may be susceptible to subtle changes in internal solution composition depending on their postnatal age.

Across a range of neuronal phenotypes, evidence points towards divergent effects of the internal solution on neuronal dynamics (Robbins et al., 1992; Spigelman et al., 1992a; Zhang, 2004). Studies on pyramidal neurons in the hippocampus have revealed the importance of subtle changes in internal solution on the electrical characteristics of patched cells (Kaczorowski et al., 2007; Velumian and Carlen, 1999). For example, Kaczorowski et al. (2007) found that CA1 pyramidal neurons exhibited changes in neuronal excitability and intrinsic membrane properties when patched with the distinct solutions, potassium methylsulphate

(KMeth) and potassium gluconate (KGlu): KMeth resulted in decreased input resistance, AP threshold and afterhypolarisation (AHP) compared to neurons patched with KGlu. This highlights the delicate balance of ions across the cell membrane and their impact on intrinsic cell properties.

The inclusion of a dye such as biocytin or neurobiotin in the recording electrode is incredibly common in electrophysiological investigations, as it allows for post-hoc recovery of morphology of the neurons, allowing for more accurate categorization of neuronal subtype and for further investigation into dendritic and axonal arborization (Bender et al., 2003). However, few groups have investigated the molecular effects of these compounds on neuronal dynamics and development-dependent changes. This project will investigate biocytin-containing internal solution's impact on the intrinsic parameters of SS neurons across P4-P14, alongside investigation into development-dependent changes in neuronal dynamics.

1.6 Temperature's effects on intrinsic properties

Temperature is closely controlled variable in the brain, which is homeostatically regulated in *in vivo* states by the hypothalamus (Childs, 2008). In *in vitro* electrophysiology experiments, temperature is externally regulated by the researcher by warming the artificial cerebral spinal fluid (aCSF) surrounding the slice. Brain temperature of C57BL/6 mice is around 34-38^{o}C (Bejanian et al., 1991; Shoji et al., 2016) but electrophysiology investigations are routinely performed at room temperature ranging from 22-27^{o}C (Andjelic et al., 2009; Pratt and Khakhalin, 2013; Segev et al., 2016; Valiullina et al., 2016). Performing experiments at room temperature is widespread practice, yet the effects of temperature on neural dynamics are complex and non-linear. Even small fluctuations have notable impacts on neuronal functioning, with temperature-alterations impacting on both presynaptic release probability (Katz and Miledi, 1965) and presynaptic plasticity (Micheva and Smith, 2005), with lower temperatures resulting in a delay in synaptic release, exocytosis and endocytosis.

Given their dependence on ionic diffusion and molecular dynamics of ion channels/pumps, we would also expect a temperature-dependent change in the intrinsic dynamics governing action potential generation and propagation. Indeed, the early investigations of Hodgkin and Huxley demonstrated that temperature has profound effects on *in vitro* slice electrophysiology (Hodgkin and Huxley, 1952) and significant impacts on the intrinsic properties of neurons. Since these investigations, there have been multiple reports of the effects of temperature on neural dynamics across widespread areas of the brain. Both neurons in the cortex (Buchhalter and Dichter, 1991; Lee et al., 2005; Thompson et al., 1985; Volgushev et al., 2000) and

hippocampus (Thomas et al., 1986) display changed intrinsic properties when slices at room temperature were subject to increases in temperature above 32^{o}C. These differences need to be taken into account when compliling big datasets and the assimilation of electrophysiology data and comparison of *in vitro* data collected at RT vs neurons operating at PT in the brain *in vivo* states.

Looking at the changes that temperature has on intrinsic properties is an interesting investigation: looking at the impact of methodological differences in electrophysiology recordings and being able to ascertain whether changes in the biophysical parameters of SS cells are due to internal solution, age, or temperature; and, additionally, whether temperature affects the pharmacology of the different internals.

1.7 Aims:

OVERALL AIM: To understand how the intrinsic properties of SS neurons in layer IV of the mouse somatosensory cortex develop, and how this implicates overall cortical network development

1. Investigate the active dynamics of spiny stellate cells throughout development, with the aim of characterizing how the AP waveform develops over the first two weeks of life; investigate and assess how the passive dynamics of spiny stellate cells mature and implicate excitability properties of the cell.

2. Compare and contrast how three distinct internal solutions, with varying ionic concentrations, affect the AP waveform and understand what this means for AP development. Investigate how the different the internals affect both the active and passive dynamic properties of cells through the first two weeks of life.

3. Investigate the effects of temperature on intrinsic properties over the course of development and across internal solutions.

Chapter 2

Methods and Materials

2.1 Electrophysiology:

2.1.1 Experimental animals

Male and female C57/Bl16 mice bred at the University of Bristol aged P4-P14 were used in this study. Mice were group housed and kept alive on an alternating light and dark 12 : 12 cycle, permitted to food and water *ad libitum*.

2.1.2 Slicing procedure

Male and female C57/Bl16 mice were scarified by UK Home Office Schedule 1 procedure (cervical dislocation). Brains were dissected and deposited in icy cutting fluid, which contains a higher concentration of Mg^{2+} (9mM) ions to reduce excitotoxic damage during slicing. Thalamocortical slices (see figure 2.1) at a thickness of 400μm were sliced with a VT1200 vibratome (Leica Microsystems, Milton Keynes, UK).

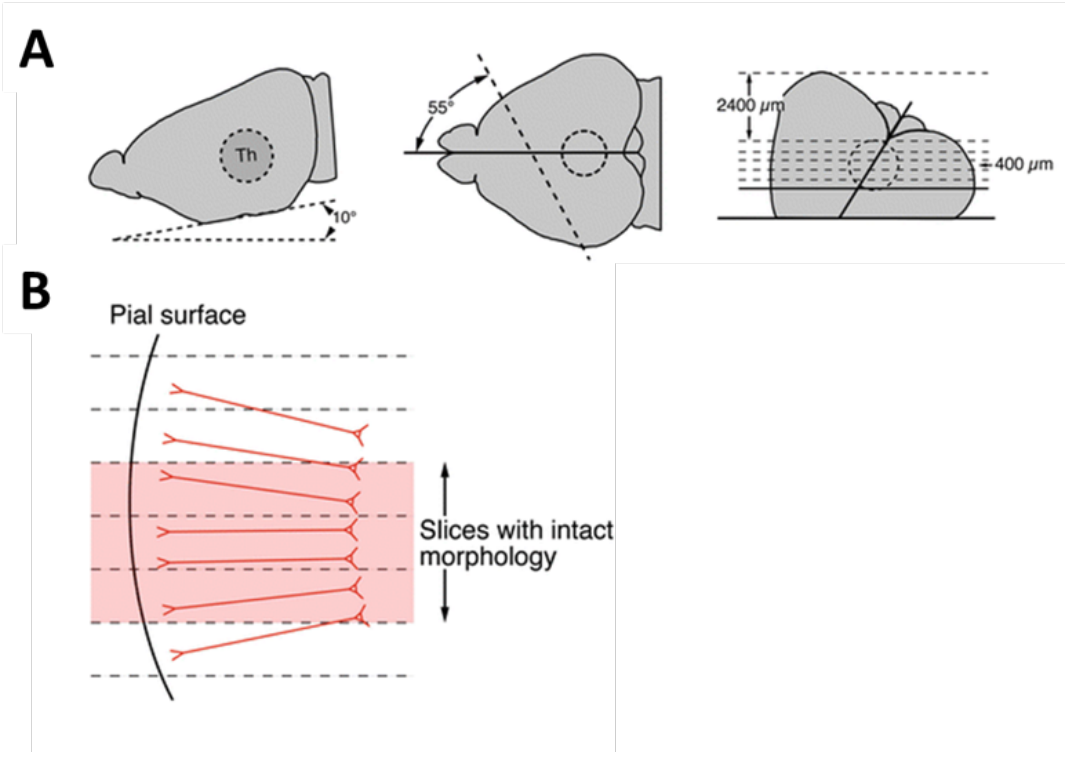

Fig. 2.1 **Thalamocortical slice procedure**
(A) The dissected mouse brain is angled down a 10° ramp, before a cut 45/55° from midline is made. (B) this slicing technique allows for visualization of barrels as well as preserved projections from the thalamus (Agmon and Connors, 1991)

2.1.3 *In vitro* patch clamp recordings

After slicing, the brain sections were moved to a beaker containing carbogen-bubbled artificial cerebral spinal fluid (aCSF), composed of 119.0mM NaCl, 2.5mM KCL, 11.0mM D-Glucose, 1.0mM $NaH_2OPO_4.H_2O$, 26.5 mM $NaHCO_3$, 1.3 mM $MgSO_47H_2O$, and 2.5mMol $CaCl_2$ and were allowed to rest for post-incubation period of at least 45 minutes at room temperature. As cell death occurs after slicing and slices are likely to be viable for a limited time period (6-12hs; Buskila et al., 2014), experiments were performed and finished within 7h post-slicing.

Post incubation, individual slices were moved to the bath, which, like the beaker, was continually perfused with aCSF bubbled with carbogen. Slices were kept at room temperature (22–27°C) throughout recordings, and a subset of experiments were performed at physiological temperature, details of which are discussed in section 2.1.3. Unnecessary movement of the brain-slice due to the suction/aCSF perfusion was prevented by implenting a 'harp' (slice hold-down; see figure 2.2) which was positioned over the brain-section so that the individual strands of the harp did not interfere with the barrels that were to be imaged. Slices were then imaged using an optical microscope (Zeiss Axioscope) using infrared DIC optics. Spiny stellate cells were identified by initially using a low power objective lens (Olympus 4x) to identify barrels in layer IV; another objective (Olympus 10x) was then used to locate spherical shaped cells, and a 40x objective lens was used during patching to as to visualise the 'dimple' indicating sufficient positive pressure.

Within the somatosensory cortex, spiny stellate cells are specific to layer IV and are found within barrels (see figure 2.2D). They are spherical in shape and are distinct from L5 pyramidal neurons which are larger and located in next cortical layer. In early development, however, it can be difficult to visualise barrels and L5 pyramidal neurons are of similar morphology. In these instances, (postnatal days P4-P7), instead of locating barrels (undistinguishable this early on), the protocol would be to either a). locate the hippocampus and work upwards b). find the edge of the cortex and count down through the distinct cortical layers to find layer IV. Hence, by either laminar location, cellular density or (at later ages) cell morphology, cell type could be confidently determined.

Patching pipettes were fire-polished pipettes and drawn borosilicate capillary glass (Harvard Apparatus, Edenbridge, UK) by micropipette puller (model P87, Sutter Instrument Co., CA, US). These were pulled so that they had tip resistances of 3-6MΩ when placed in the bath and containing the appropriate intracellular solution for patching. Internal solutions were sterile-filtered through a 0.2μm filter and then recording pipettes were backfilled with internal solution, which was kept over ice to prevent the denaturing of ATP and preserve its activity *in vitro*.

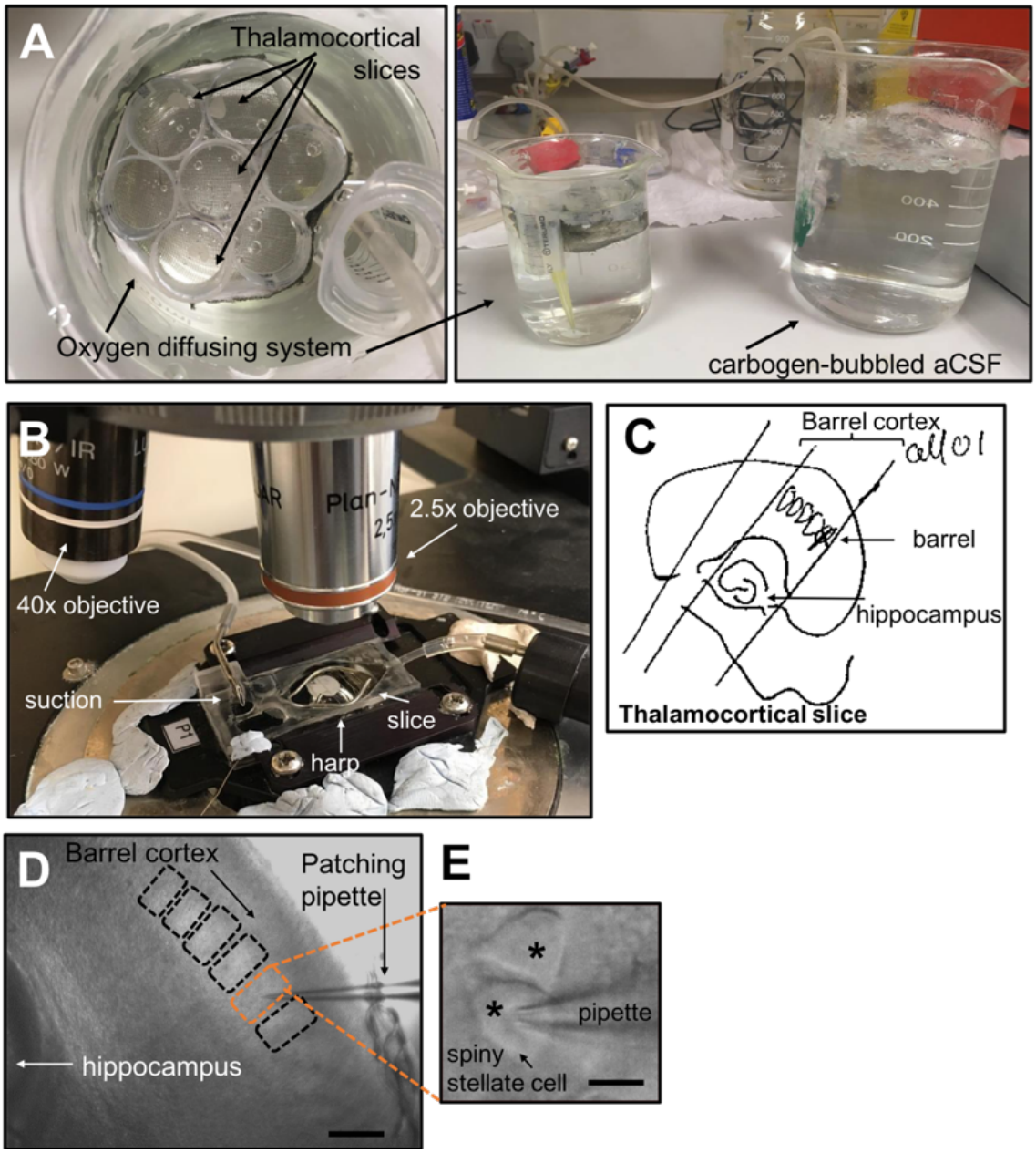

Fig. 2.2 **Experimental set-up:**
(A) Custom-made Recovery Chamber, containing carbogen bubbled aCSF that perfuses the slice (B) Experimental setup (C) sketch of thalamocortical slice as pictured in (B) from lab-book, indicating distinct slice landmarks such as barrels and hippocampus, lines of harp, and which barrel a cell was patched from (D) Low magnification IR-DIC contrast image of a thalamocortical slice, displaying the barrel cortex. The orange box shows a barrel containing SS layer 4 neurons - also in the panel to the right. Scale bar, 200 μm. (E) SS neurons at higher magnification. SS neurons marked by black asterisks. Scale bar, 10 μm.)

Once a spiny stellate neuron was identified using the optical microscope (Zeiss Axioscope), the micropipette containing the appropriate internal solution was lowered using a motorised manipulator; prior to submersion in the bath of perfused aCSF, 70-100mmHg of positive pressure was applied. Spiny stellate cells were patched clamped, obtaining gigohm resistance tight seals ahead of break-in. Capacitance was compensated via automatic headstage function. Signals were amplified using a MultiClamp 700B amplifier (Molecular Devices, Unon City, CA), digitised using an Micro1401 data acquisition board (Molecular Devices) and stored on a personal computer using Signal software (Version 5l; Cambridge Electronic Design Ltd, UK). Recordings were low-pass Bessel filtered at 4kHz, with a sample rate of 50kHz. Artifical cerebrospinal fluid and internal solution combined causes a liquid junction potential error (~15mV) which was corrected for arithmetically in the custom-written MATLAB script to analyse the data obtained from recordings.

2.1.4 Temperature experiments

For a subset of experiments investigating the effect of temperature on intrinsic properties, aCSF perfusing the slice was heated with a thermistor heater, positioned near the slice. Slices were recorded at room temperature then heated to approximate physiological temperature, and the temp of the aCSF was assessed by a feedback circuit and temperature controller. aCSF temperature underneath the lens was checked with a separate thermometer which was positioned a few mm away from the slice.

2.1.5 Internal solutions

Distinct internal solutions were used, the details of which can be found in Table 2.1-3. All components for internals were obtained from Sigma-Aldrich Ltd. (Dorset, UK). The pH of each internal solution was corrected using potassium hydroxide to 7.25, and osmolarity measured at 285mOsM.

Compound	Concentration (mMol)	Molecular weight (g/Mol)
$KMeSO_4$	130.0	134.2
NaCal	8.50	58.0
HEPES	5.00	238.3
EGTA	0.50	380.4
Mg-ATP	4.00	507.2
Na-GTP	0.30	523.2

Table 2.1 Standard internal, 'Internal2'

Compound	Concentration (mMol)	Molecular weight (g/Mol)
$KMeSO_4$	115.0	134.2
NaCal	8.50	58.0
HEPES	5.00	238.3
EGTA	0.50	380.4
Mg-ATP	4.00	507.2
Na-GTP	0.30	523.2
Sucrose	31.0	342.3

Table 2.2 Sucrose internal

Compound	Concentration (mMol)	Molecular weight (g/Mol)
$KMeSO_4$	115.0	134.2
NaCal	8.50	58.0
HEPES	5.00	238.3
EGTA	0.50	380.4
Mg-ATP	4.00	507.2
Na-GTP	0.30	523.2
Biocytin	31.0	372.5

Table 2.3 Biocytin internal

The Biocytin internal has reduced $KMeSO_4$ to account for the dye (therefore returning the osmotic pressure to equilibrium); it therefore made sense to create a 'control' internal to account for the addition in dye; this control comes in the form of a 'Sucrose' internal, which contained sucrose instead of biocytin.

2.2 Measuring intrinsic membrane properties of recorded neurons

For successful patch attempts on healthy spiny stellate cells, a simple current injection protocol (Protocol 1) was performed, which was programmed into Signal software (Molecular devices). Protocol 1 was a cycle of alternating hyperpolarising and depolarising 500ms square current pulses that increased in size to 0.14V. This was made up 11 current steps and was repeated on average 10-20 times per cell (see figure 2.3 below). This resulted in a dataset per patched spiny stellate neuron of around 150 frames at a sampling frequency of 50kHz, roughly equivalent to 150s per protocol.

These datasets were analysed by converting the signal files (.cfs) into Matlab files (.mat) and then using purpose-specific scripts written in MATLAB (version 6, Mathworks). Since some intrinsic parameters (such as input resistance) are voltage-dependent, after initial

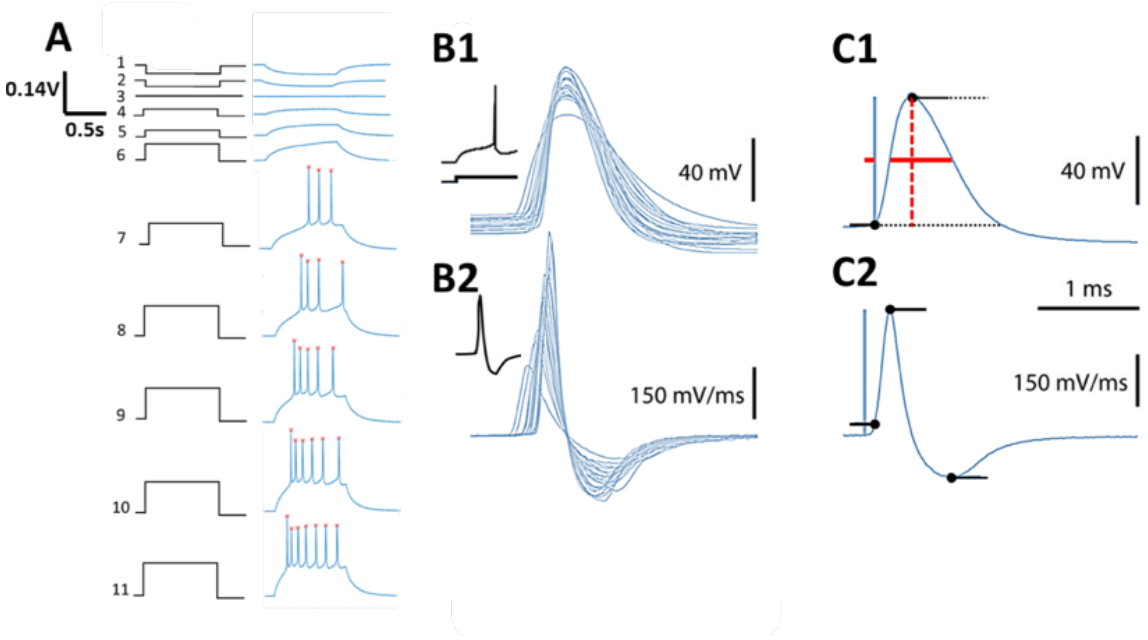

Fig. 2.3 **Current injection protocol for measuring intrinsic properties**
(A)Voltage responses of a patched SS neuron to the current injection protocol - 11 steps of current of duration 0.5s with an initial hyperpolarising step and successive depolarising steps. Red crosses indicate AP detection detected by MATLAB script. (B1) Individual action potential waveforms from spiny stellate neurons overlaid and aligned by peak. Inset shows the first AP (in figure A, step 7); the first AP is recognised by the code when dV/dt passes 10.5 V.s^{-1} . (B2) Equivalent dV/dt traces. (C1) Single AP example with marked measurements outlined; height, width (C2) Related dV/dt trace with marked pointers to measurements taken for AP threshold, max RoR and max RoF.)

recording of the RMP, successive measurements were taken with by setting the holding potential such that the membrane potential was -70 mV.

The quality of the seal was judged upon immediately achieving whole cell access. The properties observed at this initial time point (Rest V_m, RSeries) were continually monitored throughout the experiment and later time points were compared against the initial access to see if a cell had deteriorated significantly over the course of the experiment.

If a cell was deemed to be a poor seal (usually indicated by a noisy trace), the cell was discarded; if a cell appeared to deteriorate over the course of recording (see patching quality assessment check in Section 3.3 Analysis), the cell was discarded and not included in any furtherx analysis.

Chapter 3

Analysis

3.1 Statistical Analysis

All statistical analysis to compare between different populations was performed using SPSS software (version 22.0, SPSS 2013). For all statistical tests the threshold for significance was taken as p=0.05, with data falling within 95% (p<0.05), 99% (p<0.01), or 99.9% (p<0.001) significance levels. To test for the effect of development on intrinsic properties, a one-way ANOVA was used. Two-way ANOVAs with Bonferroni correction were utilised for comparing between internal solutions. For the subset of experiments investigating temperature's effect on intrinsic neuronal properties, comparisons within cell populations at room (<27^{o}C) vs. physiological (>27^{o}C) temperature were calculated using two-tailed, paired t-tests. Significance was set at $p < 0.05$. The n-values reported refer to the total number of neurons recorded. For all population data the average value used is the mean average, with the data displayed as the average ± the standard error of the mean (SEM).

3.2 Analysis of Signal files

Rigorous methods of removing anomalous data were employed by both in-assessment checks and post-experiment checks. Various cell properties were closely monitored throughout the experiment to assess the health of cell and the quality of the patch-attempt. These included visual cues and quantifiable measures of cell health: e.g.

3.2.1 Patching Quality Assessment check

- **Intrinsic properties (RSeries, Vm):** these were measured upon initially achieving whole cell access and throughout the experiment – cells that showed significant changes

in Rseries (+/- 20%) or Resting membrane potential were considered to be deteriorating in patch-quality and or cell health, and hence were discarded from future analysis.

- **Cell morphology:** If the cell appeared to change shape during the recording, or if the nucleus enlarged, or if the pipette appeared to drift and this corresponded with one or more changes in intrinsic properties, the experiment was aborted and a new spiny stellate neuron sought.
- **Cell death:** If a cell died during the experiment and stopped firing, this was noted and the cell was not included in the analysis.
- **Spiking cells:** For active dynamic experiments only cells that elicited action potentials were included in the analysis.

3.3 Summary of passive dynamic properties

- **Resting membrane potential (mV):** taken as the average membrane voltage (Vm) in the when current injection was not applied, immediately after entering current-clamp mode.
- **Input Resistance (MΩ):** the difference between the Vm at its SS-voltage and the amount of current injected
- **Membrane time constant (ms):** first order- exponential fit to the membrane charging curve in the first hyperpolarising trace of Protocol 1

3.3.1 Intrinsic membrane properties

When measuring the intrinsic properties of cells, the very first (initial hyperpolarising) step in Protocol 1 was analysed. To measure properties such as Ri and $/tau_m$, a single exponential decay was fitted to the hyperpolarising voltage decay curve.

3.3.2 Input Resistance and the membrane time constant:

Input resistance is defined by Ohm's law:

$$V = I \times R \tag{3.1}$$

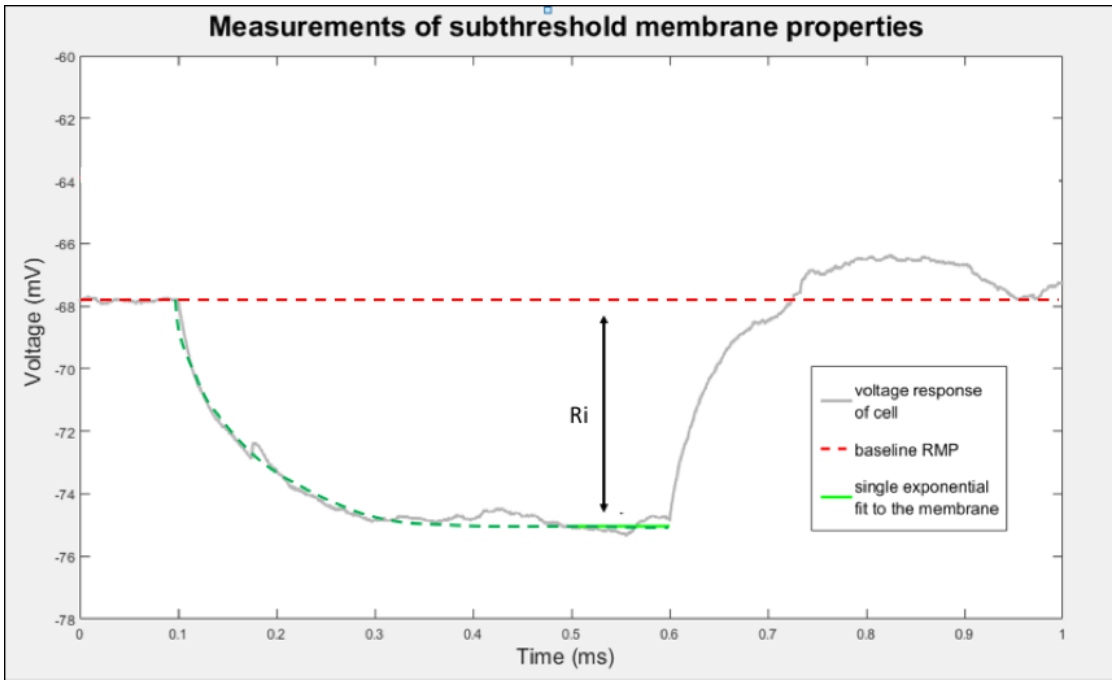

Fig. 3.1 **Current injection protocol for measuring intrinsic properties**
(A)Voltage responses of a patched SS neuron to the current injection protocol - 11 steps of current of duration 0.5s with an initial hyperpolarising step and successive depolarising steps. Red crosses indicate AP detection detected by MATLAB script. (B1) Individual action potential waveforms from spiny stellate neurons overlaid and aligned by peak. Inset shows the first AP (in figure A, step 7) ; the first AP is recognised by the code when dV/dt passes 10.5 V.s^{-1} . (B2) Equivalent dV/dt traces. (C1) Single AP example with marked measurements outlined; height, width (C2) Related dV/dt trace with marked pointers to measurements taken for AP threshold, Max RoR, and Max RoF)

And it can be calculated experimentally by finding the difference between the membrane potential at its steady state voltage and the amount of current injected, as defined by the following formula:

$$R_i = \frac{\Delta V}{\Delta I} \tag{3.2}$$

This formula reflects how a greater input resistance will yield a larger change in voltage in reaction to a current injection. Since τ_m can be estimated by fitting an exponential to the membrane charging curve, capacitance of the cell membrane (C_m) can be approximated with the following formula:

$$C_m = \frac{\tau_m}{R_i} \tag{3.3}$$

If we assume the neuron in question is spherical, input resistance would approximate 'membrane resistance' (see figure 3.2 for a schematic of this). This approximation relies upon the idea that the resistance between neuronal membrane and the electrode (the 'Seal' resistance, RSeal) and the resistance of electrode itself, is negligible. In reality, a neuron has an axon and dendrites as well as spherical soma which makes things more complicated.

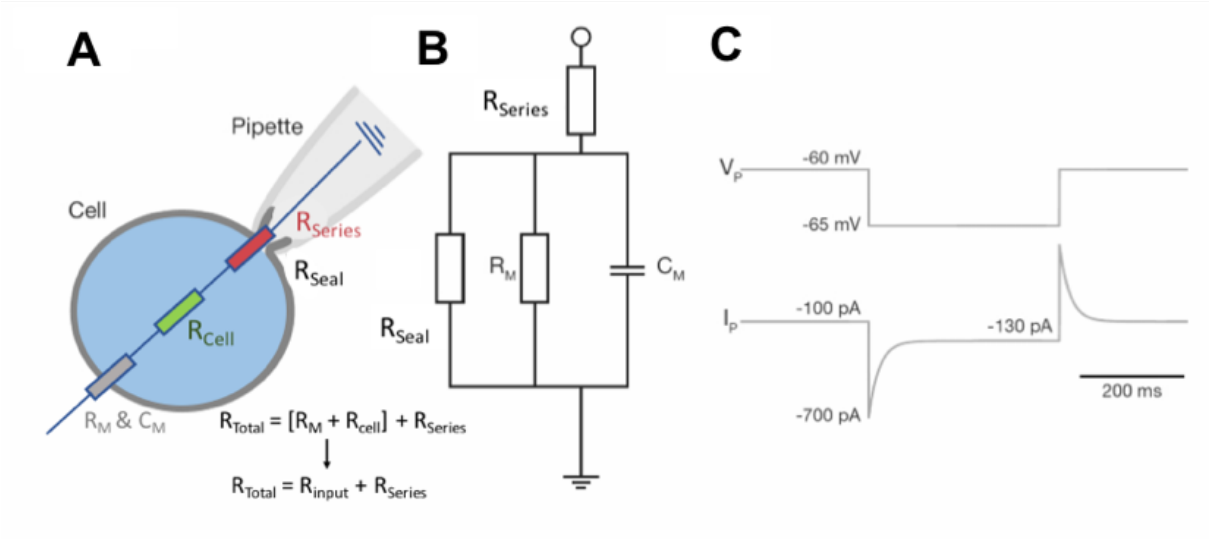

Fig. 3.2 **Modelling the neuron as a sphere | 'whole-cell' configuration of a neuron** (A) Diagram demonstrating series resistance (R_{series}) in series with a parallel circuit of resistance of the gigaohm seal (R_{seal}), the R of the cytoplasm of the cell (R_{cell}) resistance of the membrane (R_m) and the membrane capacitance (C_m) (B) Electrical circuit diagram of schematic in (A). (C) Corresponding voltage (top trace) and current trace (bottom trace) depicted in whole cell configuration.)

Membrane capacitance

Since accurate measurements of capacitance rely upon on valid measurements of the τ_m and R_i, calculations of capacitance have been omitted from this report as they would be estimations only. In principle, to evaluate the overall membrane capacitance of a cell, the formula $C_m = \frac{\tau_m}{R_i}$ is used (Bear, 2007).

3.4 Analysis: Active dynamics

For measurements of various active dynamic properties, only the first action potential of each trace was used. e.g. if there are 11 current steps, and the first action potential fired is on the 6^{th} step; this is the action potential measured. This was done to reduce errors that could accrue from the adaptation of APs during trains; when 'burst' firing of neurons is seen, action potentials often get smaller in successive current trains. As this investigation focuses on the changes to the AP properties (such as height and width) across development, it was important to select only the first AP from each current sweep and keep this consistent throughout analysis.

For active dynamic properties, the first AP generated in a series of 11 depolarising square wave current steps of size 0.04V (Protocol 1) was used. For passive membrane properties, the initial hyperpolarising step in Protocol 1 was used. Results were obtained by purpose-specific MATLAB scripts.

3.4.1 Summary of active dynamic properties

- **Action potential threshold (mV):** measured by taking 1st derivative of the voltage trace against time (dV/dt) and finding the first instance where value of dV/dt surpasses 10.0mV.s^{-1}. For data on AP threshold, the average was calculated per current train.
- **Action potential peak (mV):** absolute voltage of the AP waveform
- **Action potential height (mV):** Absolute voltage pinnacle of the AP waveform minus the AP threshold
- **Action potential width (ms):** the half-amplitude of the AP height with linear interpolation between samples
- **Maximal rate of rise (mV.s^{-1}):** maximum value of dV/dt of the AP waveform
- **Maximal rate of fall (mV.s^{-1}):** minimum value of dV/dt of the AP waveform.

3.4.2 Action potential threshold, maximum rate of rise and fall and height and width

One way to examine the active dynamics of APs is to use the dV/dt and plot this against the membrane potential (otherwise known as a phase plot) in order to understand the kinetics of APs (Jenerick, 1963). The advantage of viewing the spike waveform like this is that it

is immediately evident where the AP threshold occurs; the voltage at which dV/dt rapidly increases (see figure 3.4.2B). A MATLAB script was written to determine AP threshold by taking dV/dt of the voltage trace and calculating threshold by determining when the value of dV/dt was greater than 10.0mV.s^{-1}; this value corresponds to the AP threshold measured in mV, reflected in figure 1.1. The maximum rate of rise (max RoR) is the maximum value of dV/dt of the AP waveform; it is the part of the AP waveform with the largest gradient; the Min dV/dt is defined as the largest gradient of the decreasing slope; both are marked on the phase plot below (figure 3.3B). AP height is defined the difference between the peak of the AP waveform and the AP threshold, and AP width is measured as the divergence between the increasing and decreasing slopes of the AP waveform at half-height; these can been seen in figure 3.3A.

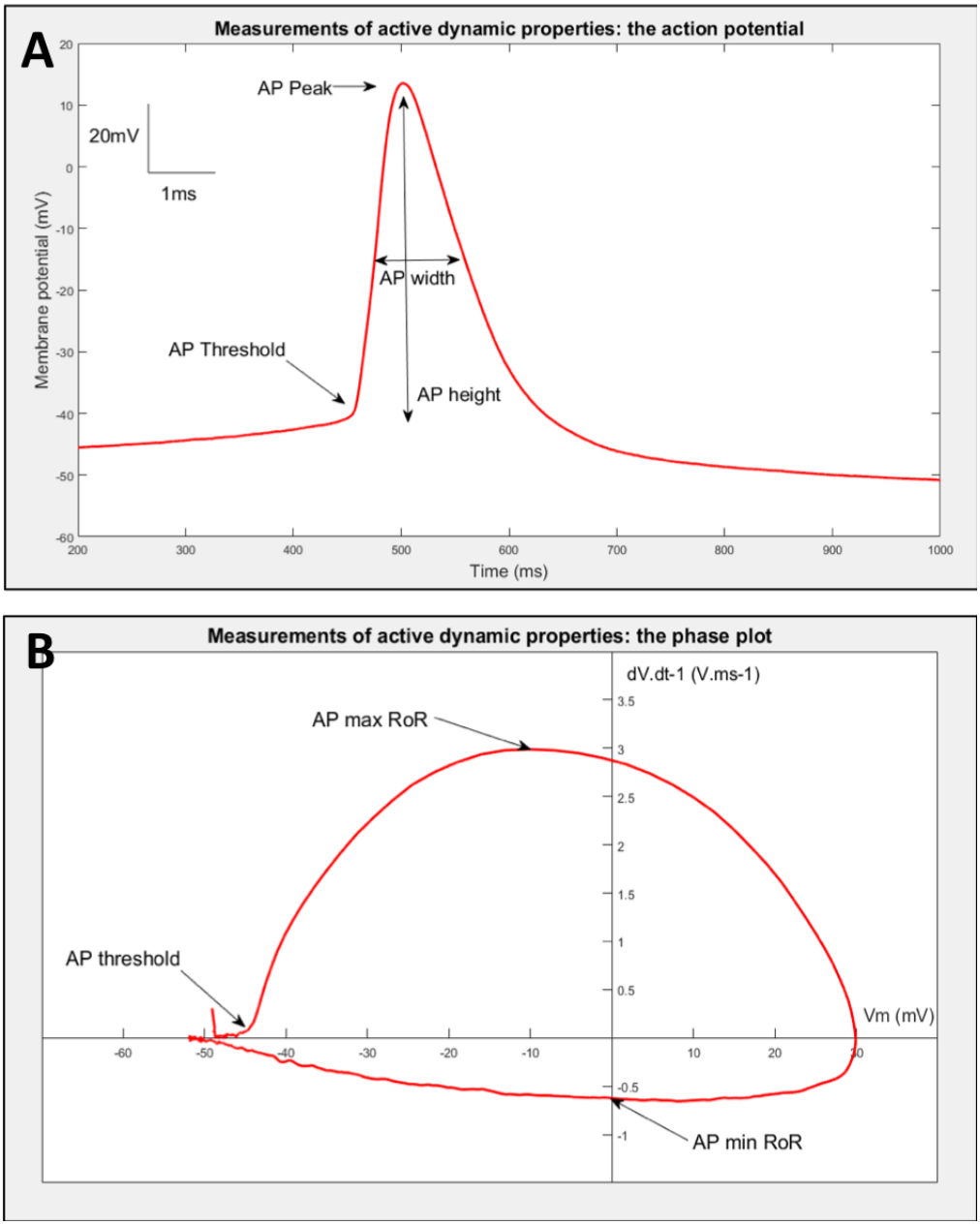

Fig. 3.3 **Measurements of active dynamic properties in MATLAB.**
Representative AP waveform (A) and corresponding phase plot (B); first derivative of the waveform against membrane potential) from a P10 spiny stellate neuron showing measurements of AP peak, height, width at half height, AP threshold and AP maximum and minimum rate of rise)

Chapter 4

Results

4.1 Introduction

Action potentials were produced from a total of 78 out of 91 LIV spiny stellate cells; this was from a cohort of 32 WT C57/Bl16 mice, with 1-4 animals used per age group. This chapter will be split into 3 sections, with the first examining how the intrinsic properties of spiny stellate neurons change with postnatal age (focusing on the standard internal dataset), the second examining how different internal solutions affect various intrinsic properties, and the third looking at how temperature affects intrinsic dynamics.

4.2 Maturation of intrinsic properties in spiny stellate cells

The data presented in this section is from the standard internal ('Internal2') dataset, where recordings were taken at room temperature. A total of 37 spiny stellate neurons were patched with a standard internal ('Internal2') from 15 slices and 11 mice. Day-by-day data is shown.

The development of electrophysiological properties of neurons has been researched across many areas of the cortex, from the anterior cortex (Pan et al., 2016); to the visual cortex (Etherington and Williams, 2011; Kasper et al., 1994); prefrontal cortex (Zhang, 2004); auditory cortex (Oswald and Reyes, 2008) and to our region of interest, the somatosensory cortex (Valiullina et al., 2016). There seems to be a common theme in the maturation of neuronal dynamics across these regions, with ageing leading to taller and faster APs, lower R_i and a more hyperpolarised RMP. Few reports examine in detail the maturation of intrinsic properties in SS cells in mouse barrel cortex however. Since neurons are at the hub of key sensory input processing for the cortex, studying these changes over the critical period

for synaptic plasticity will help us gain greater understanding about the key changes that underpin healthy neuronal functioning in adult cortical networks.

4.2.1 Passive dynamics of spiny stellate neurons across the first 2 weeks of life

While a few previous studies have demonstrated alterations in passive membrane properties during postnatal development (Ehrlich et al., 2012; Etherington and Williams, 2011; McCormick et al., 1985; Oswald and Reyes, 2008; Valiullina et al., 2016; Zhang, 2004) none have investigated in detail the properties of SS cells in the mouse barrel cortex. The following section describes the developmental changes between P4 and P14 of passive dynamics of layer IV SS cells measured using current clamp electrophysiology. Intrinsic membrane properties were recorded from 37 SS neurons.

Between P4 and P14, there appeared to be a slight hyperpolarisation of resting V_m measured immediately after whole cell break-in, though this did not approach significance ($p>0.05$; one-way ANOVA, see table 4.1C). Resting Vm was more depolarised at P4 with a mean of -61.6 ± 5.92 -mV compared to that at P14 which had a mean V_m of -71.5 ± 2.02mV ($p<0.05$; Tukey-Kramer single-step multiple comparison test). This could, however, be due to these small, immature neurons having a high membrane resistance and shunting conductance (a phenomenon that occurs via the gigaseal formation in whole-cell recordings); a more reliable way of measuring the RMP could be to use cell-attached configuration of NMDAR-dependent single channel currents, as performed in other investigations of early intrinsic properites (Yakovlev et al., 2013).

There was a progressive decrease in R_i between P4 and P14 ($p<0.05$; one-way ANOVA). The difference in R_i from P3 became evident at P10 ($p<0.05$; Tukey-Kramer single-step multiple comparison test). There was substantial variability between cells patched on the same day, notable examples being at P4 where R_i at resting V_m ranged from 346 to 885MΩ and at P10 where R_i ranged from 143 to 545 MΩ. This variation was independent of age, as tested by Levene's test of variance ($p>0.05$). Given that not all cells were sliced-matched, animal-to-animal variation could account for the range seen, but equally this result reflects the natural variation seen between cells from the same populations.

There was a slight decrease in τ_m between P4 and P14 recording at resting V_m, though this was not statistically significant ($p=0.09$; one-way ANOVA).

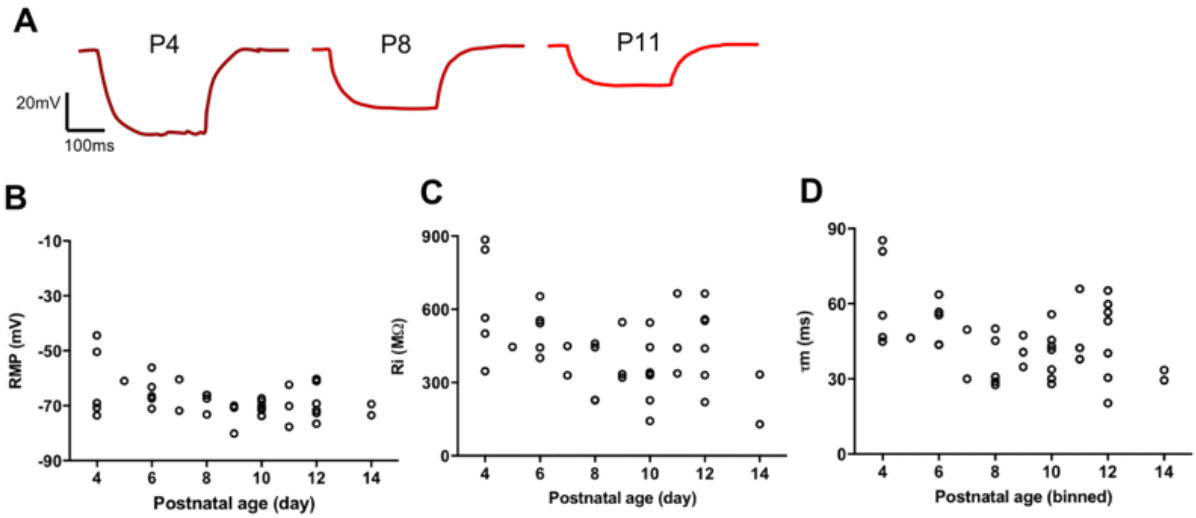

E

Postnatal age (day)	RMP (mV)	Ri (MΩ)	τm (ms)	N
4	-61.6 ± 5.92	629 ± 103	62.6 ± 8.57	5
5	-61.0 ± 0.00	446 ± 0.00	46.3 ± 0.00	1
6	-64.9 ± 2.53	519 ± 44.6	52.6 ± 3.92	5
7	-66.1 ± 5.69	390 ± 59.8	39.8 ± 9.80	2
8	-68.2 ± 1.69	340 ± 64.9	36.5 ± 4.64	4
9	-73.6 ± 3.25	334 ± 7.70	40.9 ± 3.64	3
10	-70.8 ± 0.93	320 ± 55.2	39.7 ± 3.69	5
11	-70.1 ± 4.43	482 ± 96.8	48.7 ± 8.70	3
12	-67.5 ± 2.51	420 ± 65.1	46.5 ± 6.27	7
14	-71.5 ± 2.02	232 ± 102	31.5 ± 2.02	2
P	0.3787	0.0429	0.0935	

Fig. 4.1 **Input resistance decreases with postnatal age**
(A) Example hyperpolarizing step trace taken from a P4, P8 and P11 spiny stellate neuron (B-D) Scatter plot represents RMP (left) and the τ_m (right) against animal age; each circle is an individual patched SS neuron. (E) Table presenting the changes in passive dynamics across the first 2 weeks with mean ± SEM for each day quoted; there was a significant difference in R_i ($p < 0.05$; one-way ANOVA).

4.2.2 Active dynamics of spiny stellate neurons across the first 2 weeks of life

The following section describes the developmental changes between P4 and P14 of active dynamic properties using whole cell in vitro electrophysiology.

There were clear developmental alterations in the size and kinetics of APs evoked by depolarising current injection. Analysis of maximum dV.dt and minimum dV.dt revealed a strong rate increase with age. Maximum rate of rise increased dramatically from a mean of 56.9 ± 17.3 V.s^{-1} at P4 (n=5) to 169 ± 31.3V.s^{-1} at P14. The maximum rate of fall (min dV.dt) decreased from a mean of -17.7 ± 3.60V.s^{-1} at P4 to -56.5 ± 17.0V.s^{-1} at P14. The mean minimum rate of fall does not become significantly different from P3 until P10 ($p<0.01$; Tukey-Kramer single-step multiple comparison test. Action potential threshold did not appear to decrease over the first 2 weeks ($P>0.05$; one-way ANOVA).

Action potential height dramatically increases during P4 and P14 (from 39.5 ± 3.15mV to 71.1 ± 1.23mV). Post-hoc analysis revealed that AP height became significantly different from P4 at P11 ($p<0.01$; Tukey-Kramer single-step multiple comparison test). AP width by contrast decreases over the course of development, from 7.02 ± 0.98ms at P4 to 1.14 ± 0.16ms at P14.

Maximum dV.dt became statistically different from P4 at P9 ($P<0.05$; Tukey-Kramer single-step multiple comparison) where for minimum dV.dt the statistical significance occurs later in the developmental trajectory (P11).

The results presented here display the refinement of passive and active dynamics over the course of development, with biophysical optimisations allowing for more efficient firing in mature spiny stellate neurons.

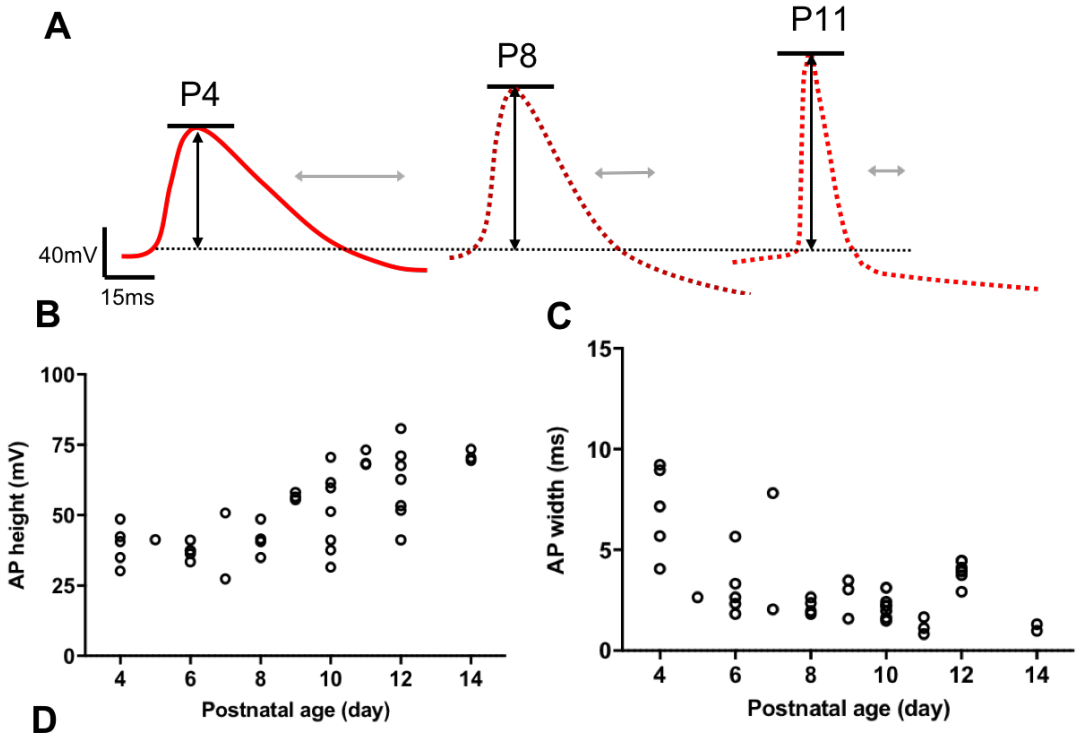

D

Postnatal age (day)	AP height (mV)	AP width (ms)	N
4	39.5 ± 3.15	7.02 ± 0.98	5
5	41.3 ± 0.00	2.64 ± 0.00	1
6	37.1 ± 1.23	3.15 ± 0.67	5
7	39.1 ± 11.7	4.94 ± 2.89	2
8	41.4 ± 2.79	2.20 ± 0.19	4
9	56.7 ± 0.77	2.70 ± 0.57	3
10	50.5 ± 5.49	2.15 ± 0.21	5
11	69.9 ± 1.68	1.20 ± 0.25	3
12	61.2 ±5.06	3.94 ± 0.20	7
14	71.1 ± 1.23	1.14 ± 0.16	2
P	0.0001	<0.0001	

Fig. 4.2 **Active dynamics change with postnatal development**
(A) Example AP waveforms taken from different age points that demarcate the start of age groups P4 (Young) P8 (Middle) P11 (Old). Scatter plot represents Ap height (B) and width (C) against animal age; circles represent individually patched cells. (D) Table presenting the changes in AP waveform across the first 2 weeks with mean ± SEM for each day quoted; there was a significant increase in AP height (***) and decrease in AP width (****) across the first two weeks (one-way ANOVA).

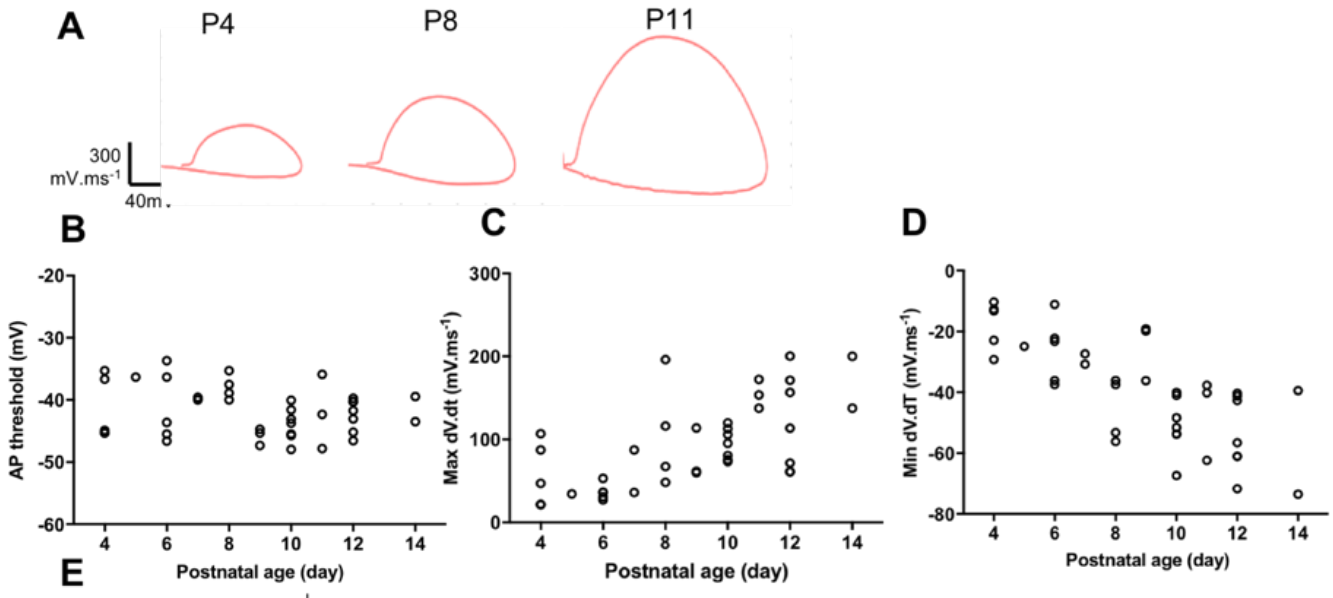

E

Postnatal age (day)	AP threshold (mV)	Max dV.dt (ms.ms^{-1})	Min dV.dt (ms.ms^{-1})	N
4	-40.5 ± 2.65	56.9 ± 17.3	-17.7 ± 3.60	5
5	-36.3 ± 0.00	34.4 ± 0.00	-24.9 ± 0.00	1
6	-41.6 ± 2.68	36.8 ± 4.45	-26.0 ± 4.88	5
7	-39.8 ± 0.20	61.8 ± 25.6	-29.1 ± 1.71	2
8	-37.9 ± 1.01	107 ± 33.0	-45.7 ± 5.21	4
9	-46.0 ± 1.30	78.5 ± 17.6	-25.1 ± 5.56	3
10	-43.9 ± 1.01	94.8 ± 7.08	-50.8 ± 3.49	5
11	-42.1 ± 3.46	155 ± 10.0	-46.8 ± 7.84	3
12	-42.4 ± 1.00	119 ± 21.7	-53.5 ± 4.62	7
14	-41.5 ± 2.02	169 ± 31.3	-56.5 ± 17.0	2
P	0.2214	0.0025	0.0002	

Fig. 4.3 **Rate of rise and and fall of action potentials change with postnatal development** (A) Example AP phase plots taken from different age points that demarcate the start of age groups P4 (Young) P8 (Middle) P11 (Old). Scatter plot represents AP threshold (B) the max RoR (C) and Max RoF (D) against postnatal age, each circle being the datapoint for an individual cell patched. (D) Table presenting the changes in active dynamics across the first 2 weeks with mean ± SEM for each day quoted; there was a significant difference in AP Max RoR ($P<0.01$) and Min RoF ($P<0.001$) across the first two weeks (one-way ANOVA).

4.3 Comparison of internal solutions across postnatal development.

Biocytin is frequently used by electrophysiologists for intracellular staining of neurons. It has high solubility and iontophoresis properties (Horikawa and Armstrong, 1988), making it an incredibly useful compound to investigate the structure of neurons. However, there has been little consideration paid to the effects of biocytin on neuronal dynamics. Using the model of SS neurons in mouse barrel cortex, the investigation aimed to address the above question with *in vitro* whole cell electrophysiology. Given that the intrinsic properties of these cells govern their excitability and functional ability to process electrical signals, seeing how the internal solution affects these properties is of interest for the validity of electrophysiology protocols.

These experiments were designed to test the impact of biocytin on the intrinsic dynamics of spiny stellate neurons. A standard internal solution (Internal2) was used as a control, alongside a Sucrose-based internal solution (to account for the reduction in $KMeSO_4$ in the internal solution in the biocytin internal and to test whether this reduction had any effects on neuronal dynamics). Biocytin comes with the added benefit of allowing for reconstruction of individual spiny stellate neurons (Bender et al., 2003; Bystron et al., 2008; Kingsbury and Finlay, 2001; Ruiz et al., 2001) which would be an interesting development of this work. For the comparison of internal solutions, recordings were binned according to distinct developmental time points into the following 'Young', 'Middle' and 'Old' bins (P4-P7; P8-P10; P11-P14). The rationale for binning the ages was to allow for easy comparison between internal solutions across P4-P14, avoiding the confounding effect of age; the age groups were not randomly assigned and were instead chosen to replicate the distinct milestones in neuronal development. This could therefore provide a better reflection of biophysical changes happening in the cell which shape functional maturation.

- **P4-P7:** The distinct cortical 'barrel' map does not form until P4 (rice and Loos, 1977), and so patching before this date would mean a degree of ambiguity as to whether spiny stellate cells were being patched. The first postnatal week is an incredibly plastic period and P7 demarcates the closing of the CP for LTP (Isaac et al., 1997) hence it is expected that significant changes would be seen between this early age period compared against later time points.

- **P8-P10:** This 'Middle' age-group is a period of rapid increase in local, recurrent connectivity in layer IV. By P8, the classical 6-layer architecture of the cortex is complete and between ages P8-P9 there is in an upsurge of local connectivity due to

unsilencing via insertion of AMPARs into newly formed dendritic spines (Ashby and Isaac, 2011). By P10, stellate cells are considered 'morphologically' mature (Callaway & Borrell, 2011).

- **P11-P14:** P11 demarcates the start of the CP for layer IV to II/III synapses and this is where information from the whiskers corresponds to an elevation in the strength of synapses (Stern et al., 2001; Lendvai et al., 2000). Around P13 is when mice begin to open their eyes and display active 'whisking' behaviour to explore their environment; this corresponds to prominent alterations in membrane-related dynamics of excitatory brain cells in the barrel cortex, with a shift from large-amplitude responses in quiescent periods, to high frequency fluctuations during movement of the mouse's whiskers (Crochet and Petersen, 2006).

These changes illustrate how membrane dynamics are related to behaviour; as the pups are ageing it is likely that these developmental milestones will be having an impact on the intrinsic properties of neurons within cortical networks.

4.3.1 Passive dynamic properties of cells patched with different internal solutions

The data obtained indicated that while some passive membrane properties were unaffected by internal solution composition, other properties were. Cells patched with across all three different internals displayed no change in their RMP. In contrast, both the input resistance and membrane time constant of cells were affected by internal solution at a specific age window.

For membrane time constant, a significant difference was seen at P11-P14 between cells patched with the standard internal and biocytin ($p<0.05$; two-way ANOVA, Bonferroni correction), with biocytin causing a decrease in τ_m; with the average τ_m for P11-P14 patched with Internal2 (44.5 ± 4.38) being almost double the τ_m for biocytin patched cells (23.0 ± 3.31). A similar change was found with input resistance ($p <0.05$; two-way ANOVA, Bonferroni correction) with the average input resistance for P11-P14 patched with Internal2 (444 ± 45.1) being significantly higher than the input resistance for biocytin patched cells (259 ± 37.9). It is not obvious why changes were only seen during the more 'mature' cells, or why resting membrane potential was unaffected.

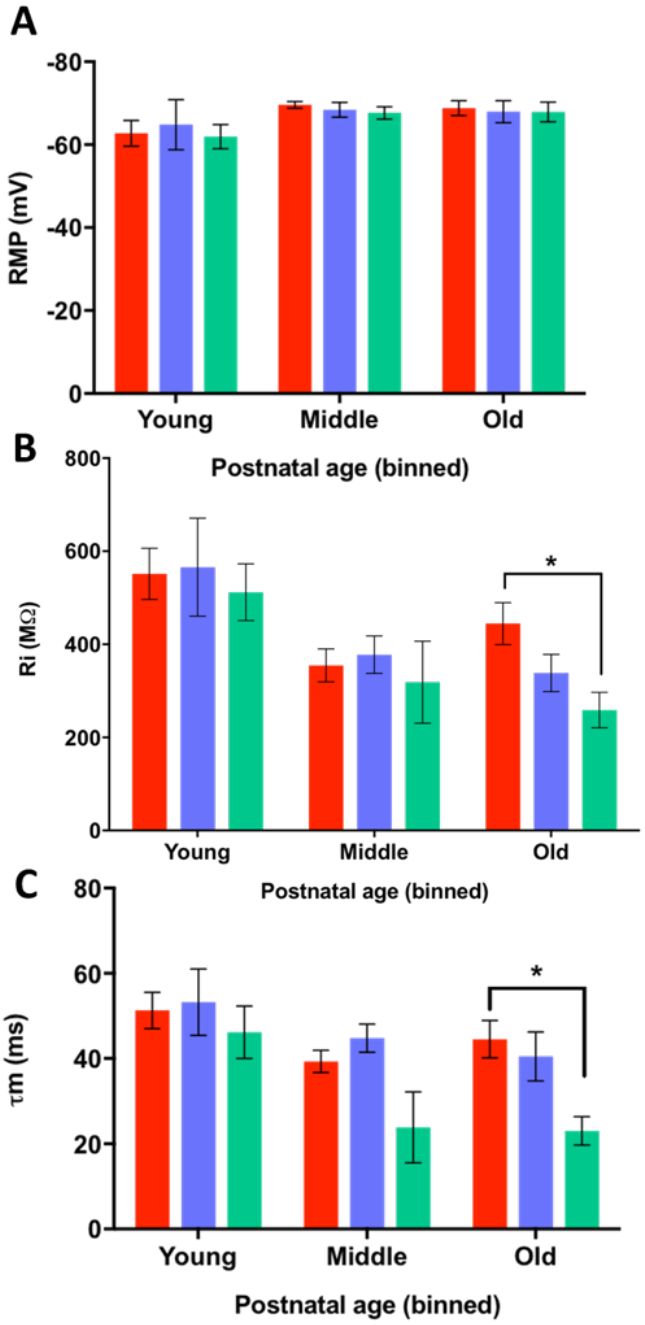

Fig. 4.4 **Comparison of passive properties across internal solutions**
Summary bar graphs displaying mean ±SEM for different passive membrane properties for cells patched with distinct internal solutions. Internal2 data in red (n=37), Sucrose in blue (n=25) and biocytin in green (n=16). (A) RMP showed no significance between internals at any age ($p > 0.05$). (B) ri, differences found between Biocytin and Internal2 dataset at P11-P14 ($p < 0.05$) (C) τ_m, significance difference found between Internal2 and Biocytin patched cells ($p < 0.05$).

4.3.2 Active dynamic properties of cells patched with different internal solutions

Greater changes were seen in the active dynamic properties of cells patched with distinct internals, with both significant differences found in the rate of rise and fall of APs, AP width and AP height between biocytin and internal2 patched cells. Only AP threshold remained unaffected.

A two-way ANOVA was conducted that examined the effect of internal solution and age on active dynamics. Simple main effects analysis showed that internal solution had an impact on AP height in the old age group ($p = 0.046$), but there were no differences between internals in the young ($p = 0.465$) or middle group ($p = 0.793$). By contrast, for AP width an opposing pattern emerged: internal solution appeared to impact AP width at young age points ($p = 0.008$) and middle ($p = 0.047$) but no significant differences were found by P11-P14 ($p = 0.855$).

Whilst alterations in input resistance, membrane time constant, AP height and maximum rate of rise were not seen until the old group (P11-P14), differences between internals were found in AP width as early as P4-P7. It is not clear why biocytin has a development-dependent effect on both the passive membrane properties and the AP-waveform, but it could be that greater variability in early development masks any distinct changes, whereas by the second postnatal week intrinsic properties fall in set ranges. In contrast therefore to current consensus, it seems biocytin at high concentrations is not experimentally inert or innocuous; this has implications for neurophysiologists and their experimental setups.

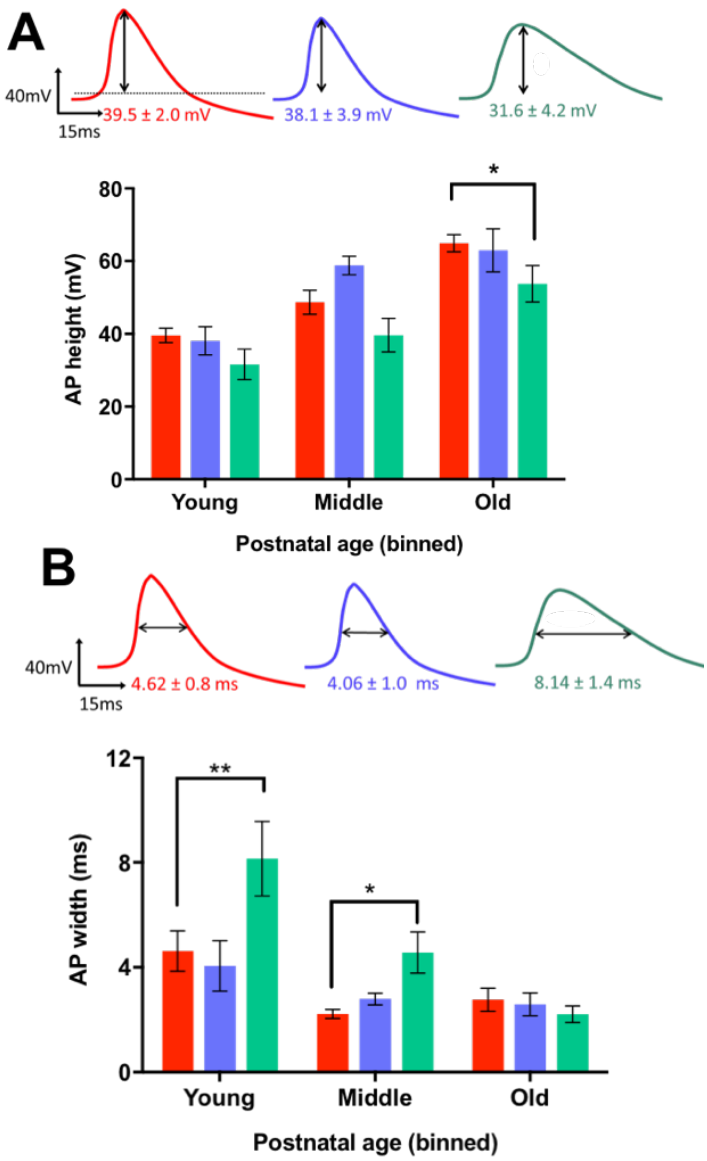

Fig. 4.5 **Biocytin affects the shape of the AP waveform:**
Example AP waveforms and summary bar graphs displaying mean ± SEM for different active dynamic properties for cells patched with distinct internal solutions. Internal2 data in red (n=37), Sucrose in blue (n=25) and biocytin in green (n=16). (A) AP height was significantly different between Internal2 and Biocytin patched cells ($P<0.05$) (B) AP width was different in the P4-P7 age group ($P<0.01$) and P8-P11 age group ($P<0.05$).

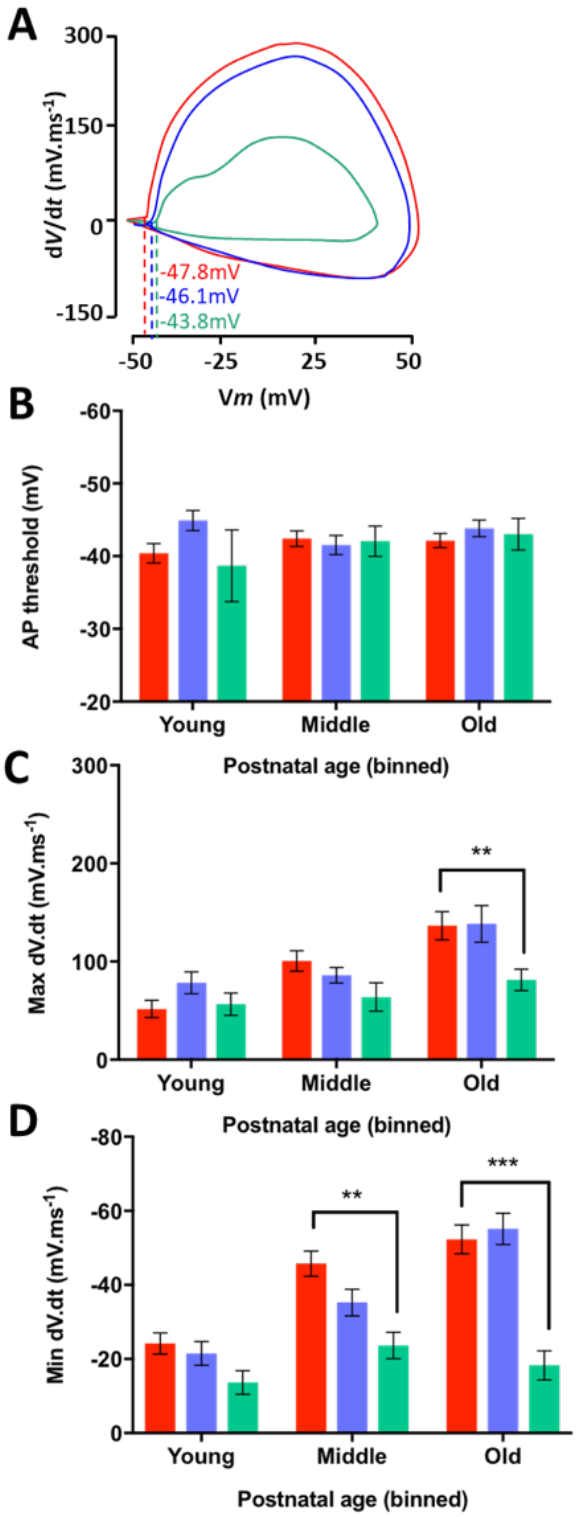

Fig. 4.6 **Comparison of internal solutions active dynamics**
Summary bar graphs displaying mean ± SEM for different active dynamic properties for cells patched with distinct internal solutions. Internal2 data in red (n=37), Sucrose in blue (n=25) and biocytin in green (n=16). (A) Example phase plane plots of a P7 cell taken from each of the internal solutions, numbers displayed are AP-threshold values for each phase-plot. (B) AP threshold showed no significance at any age ($p > 0.05$). (B)Max dV.dt, differences found between Biocytin and Internal2 dataset at P11-P14 ($p<0.05$) (C) Min dV.dt: significance differences found between Internal2 and Biocytin patched cells at the middle age point, P8-P10 ($p<0.01$) and P11-P14 ($P<0.005$).

4.4 How temperature affects intrinsic properties of spiny stellate cells

To investigate the effects of temperature on neuronal electrophysiology, a subset of experiments were performed where recorded neurons were sequentially superfused with aCSF at room and then physiological temperature. These data thereby allow consideration of the effects of methodological differences in electrophysiology recordings and to ascertain whether there are changes in the biophysical parameters of SS cells due to temperature-dependent effects on different internal solutions.

The control of temperature is not ubiquitous across laboratories, with some labs choosing to perform investigations at room temperature (22^oC -24^oC) for longevity of recordings (23^oC: Andjelic et al., 2009 ; 22^oC: Lui et al., 2018; 24^oC: Annis et al., 1993) and others choosing to approximate physiological temperature (32-37^oC) (32^oC: Miceli et al., 2013; 35^oC: (Lefort et al., 2009). It is therefore difficult to assimilate electrophysiological data across neuronal subtypes or even between distinct neuronal populations due to the disparity in lab methodology (Ferguson et al., 2014); the limitations this causes for integration of electrophysiology data is something more thoroughly discussed in Chapter 5.

Changes in as small as 5^oC can have significant effects on cell dynamics (Micheva and Smith, 2005). This makes sense when we consider the biophysics governing AP dynamics; the dynamics of the sodium and potassium ionic currents underpinning AP generation are susceptible to temperature, and early studies (Belluzzi and Sacchi, 1986; Collins and Rojas, 1982) have reported changes to the AP waveform with temperature, crediting changes to the temperature-dependence of sodium-currents.

Due to variation in temperature, recordings have been binned into two categories: $\leq 27^oC$ (room temperature - RT) or $>27^oC$ (approximating physiological temperature - PT). The mean temperature of recordings at 'room temperature' was 23.71 ± 0.5496; for physiological the mean was 34.39± 0.9669. Experiments were carried out at RT; then the bath was heated to approximate physiological temperature and the current-injection protocol was repeated. This meant that there were cell-to-cell as well as slice-by slice comparisons that could be made to allow for paired-analyses.

Analysis reveals that while temperature has a significant effect on certain intrinsic properties of spiny stellate neurons (AP height, AP Max RoR and RoF, input resistance) across all patched cells, these results are unaffected by the internal solutions used to patch cells (Internal2, Sucrose, Biocytin), indicating that the changes seen with biocytin patched cells were persistent at higher temperatures.

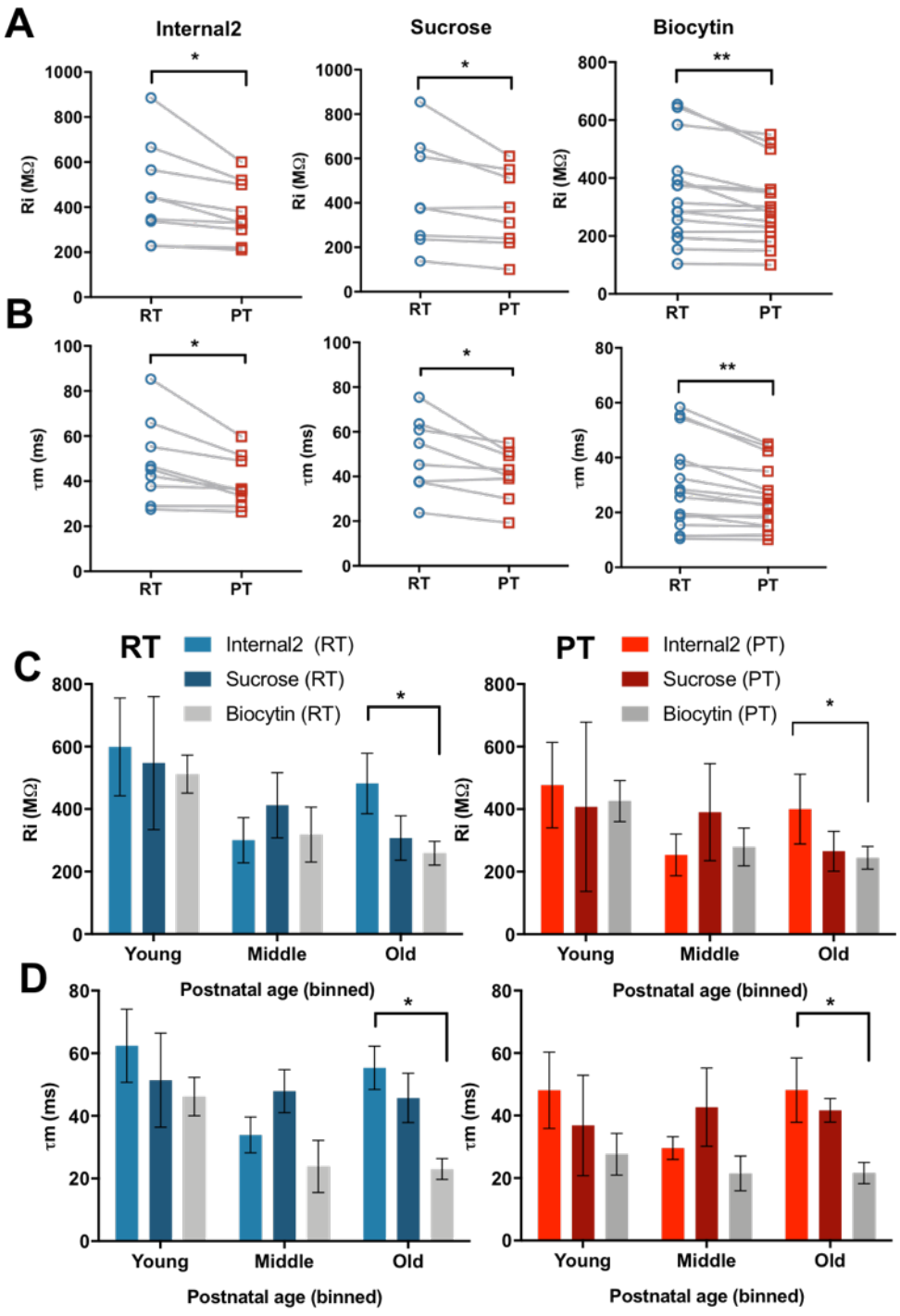

Fig. 4.7 **Temperature affects passive membrane properties**
(A-B) Changes to the passive membrane properties across each of the 3 internal solutions, Internal 2 (n=9), Sucrose (n=8), Biocytin (n=16); individual cell data is shown with cells patched at room temperature in blue and physiological temperature in red (A) displays ri, (B) displays τ_m. Significant differences found according to paired-t-tests. Summary bar charts displaying the differences between internal solutions at RT and PT; temperature of recordings did not differentially affect internal solutions.

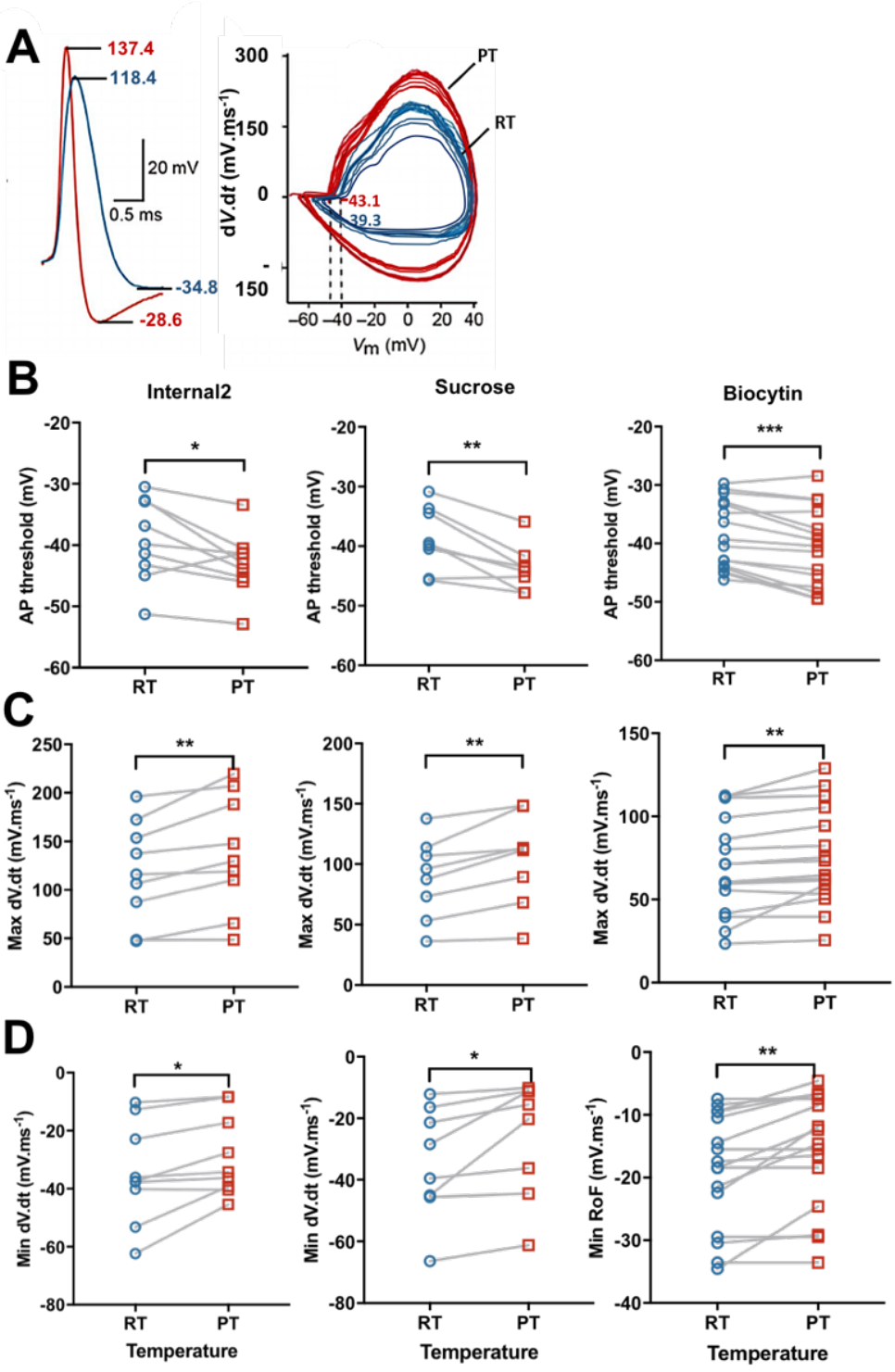

Fig. 4.8 **Temperature affects active dynamic properties of spiny stellate cells** (A) d*V*.d*t* traces, room temperature in blue and physiological temperature in red and corresponding phase plot overlaid, in panel 1 with the AP traces, the numbers in blue and red refer to the average respective values of Max RoR and RoF; in panel 2 the numbers on the phase plot refer to the average respective AP-thresholds for both RT and PT patched cells (B) AP threshold changes with temperature across each of the 3 internal solutions, Internal 2 (n=9), Sucrose (n=8), Biocytin (n=16). Significant differences found according to paired-t-tests. Increases in the rate of max RoR (C) and max RoF (D) were found across each internal dataset.

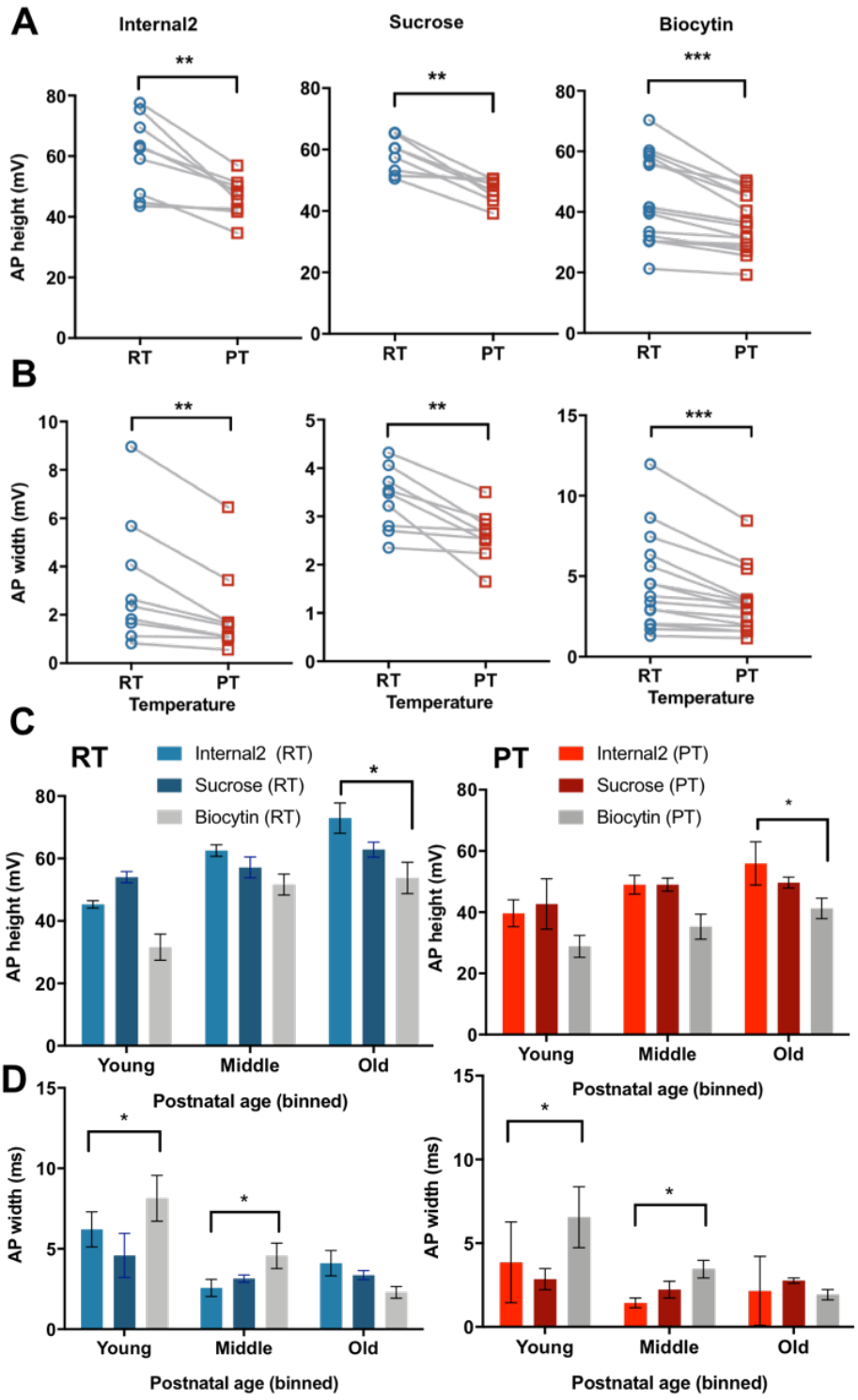

Fig. 4.9 **The effect of biocytin on AP rate of rise and fall remains at higher temperatures** Summary bar graphs displaying changes with age, internal solution and temperature (A) AP threshold does not significantly change with internal solution, age or temperature. (B). Significant differences were found between biocytin and internal2 patched cells; these changes were apparent both at room temperature and physiological temperature for both max dV.dt (B) and min dV.dt (C).

Chapter 5

Discussion

5.1 Main discussion:

The aim of this Masters was to examine how the biophysical changes shape the development of intrinsic neuronal dynamics of spiny stellate neurons across the first 2 weeks of life and understand the impact this has on the cortical circuit. Whole cell, current-clamp electrophysiology was performed to present and deliniate the electrical properties of visually identified SS cells in layer IV of the barrel cortex patched with different internal solutions across key developmental age points. A subset of data was collected to examine how temperature affects these same properties when the SS cells were patched with distinct internals. The main findings were as follows:

1. Passive dynamic properties vary across P4-P14. Input resistance decreases whereas the RMP and τ_m remain largely unaffected by postnatal age.

2. Active dynamic properties display significant alterations with development. Action potentials become faster and shorter in duration over the first 2 weeks, with corresponding increases in the rate of rise and fall. AP threshold remains unaffected.

3. Biocytin resulted in changes to both the passive and active properties of spiny stellate cells, predominantly affecting neural dynamics at later-age points. These changes persisted at higher temperatures.

4. Differences in temperature resulted in global changes to the intrinsic properties of cells, with room temperature recordings displaying increased values for R_i, τ_m , AP height, duration, rate of rise and fall and threshold.

In the first two weeks of life, neural network activity is being dramatically refined within the barrel cortex, with subtle changes in individual neurons causing large impacts on local network activity (Ashby and Isaac, 2011; Kasper et al., 1994; McCormick et al., 1985; Yuste et al., 1995). This fine-tuning is replicated in other of the cortex such as the motor cortices (Khazipov et al., 2004) and the visual cortices (Etherington and Williams, 2011).

To understand the sequence of events that shape spiny stellate cell maturation, it is important to remember that the adult phenotype is formed by a combination of genetic and epigenetic factors (Hensch, 2004). Certain changes in neuronal dynamics with age are a consequence of inbuilt genetic programming, changes in trophic factors, changes in the synaptic inputs converging on spiny stellate cells as the networks mature, and changes related to the changing morphology of the cells themselves. Particular changes in active dynamics are caused by alterations in the expression of various VICs within neuronal membranes, in addition to growth of the membrane itself as the morphology of the neuron as it develops (Kang et al., 1996; Grosse et al., 2000; Picken-Bahrey & Moody, 2003) and these will be discussed in more detail for specific intrinsic parameters.

It makes sense to see a change in the development of intrinsic neuronal properties over posnatal days 4-14 when we consider developmental time points of the mouse barrel cortex on a much broader scale. In these early days of life a number of functional developmental milestones have been reached in the mouse brain: at the end of week 1 (P7), mice begin to display active 'whisking' behaviour and thalamocortical synapses have been 'unsilenced' by the movement of AMPA receptors into the synapse (Isaac et al., 1997; Daw et al., 2007; Ashby & Isaac, 2011). By the second postnatal week (P14) and even as early as P12, the thalamocortical circuit has matured significantly; mice begin to open their eyes, hear as their auditory canal matures, and display significant increases in their arousal (Shen and Colonnese, 2016). Alterations to the neuronal dynamics result in a change in the transmission of activity through cortical networks, which in turn may be affecting (and indeed shaping) these characteristic developmental milestones in the cortex.

5.2 How do passive dynamics change over the course of postnatal development?

Input resistance was only reported statistically significant change in passive membrane dynamics with development, with immature neurons displaying significantly higher values compared to mature neurons. The values obtained in this research are comparable to other patch-clamp recordings from the somatosensory cortex in development, such as those for pyramidal neurons (557 ± 202 at P2 dropping dramatically to 81.1 ± 12.7 MΩ by P14) (Etherington and Williams, 2011) and spiny stellate neurons (Valiullina et al., 2016) and cortical neurons from rat neocortex (McCormick et al., 1985); for a comparison between the literature see table 5.1 below.

Researchers	Cell type | brain region	Immature neuronal R_i (MΩ)	Mature neuronal R_i (MΩ)
(Zhu, 2000)	Pyramidal cell | Layer V neocortex	557± 202 (P2)	81.1 ± 12.7 (P14)
(Bender et al., 2003)	Spiny stellate cell | Layer IV barrel cortex	354.2 ± 111.5 (P8-P11)	177.6 ± 65.0 (P14-P26)
(Valiullina et al., 2016)	Spiny stellate cell | Layer IV barrel cortex	596 (P4)	202 (P13)
(Daw et al., 2006)	Spiny stellate cell | Layer IV barrel cortex	402.5 ± 38.4 (P3-P5)	204.3 ± 15.0 (P19-P21)
(Conole) Present study	Spiny stellate cell | Layer IV barrel cortex	629 ± 103 (P4)	232 ± 102 (P14)

Table 5.1 Comparison table of input resistance values in development.

One role initially high R_i could be to allow immature neurons to generate APs in reaction to less frequent, weak synaptic input as circuits in layer IV are being first formed. This spontaneous activity is linked to highly synchronised activity patterns in early development, which transition to de-correlated activity in mature circuits towards a less energetically demanding neural code (Khazipov and Luhmann, 2006; Yuste et al., 1995). While it appears that spontaneous synaptic activity (in the form of mini EPSPs) increases as overall connectivity of the circuit increases (Valiullina et al., 2016), several research groups investigating the rodent barrel cortex have commented on a developmental decline in the amplitude of EPSPs

alongside decreasing input resistance of the cell (Etherington and Williams, 2011; Frick et al., 2007). As such we suggest that the change in input resistance from high to low reflects the reduction in spontaneous activity as the circuit transitions from an immature state to a mature one, with experience-dependent activity driving the desynchronization of the cortical network (Golshani et al., 2009). The pronounced reduction occurring at P10 coincides with the CP for synaptic strengthening between layer IV to II/III synapses (Erzurumlu and Gaspar, 2012; Lendvai et al., 2000; Stern et al., 2001) so could be due to intrinsically programmed changes in the cell occurring during this critical period, or due to the whisking behaviour of mice at this time impacting on the cortical circuit.

The RMP did not significantly alter over P4-P14. This is in contrast to previous literature, which reports a general decrease in RMP as neurons mature – increased hyperpolarisation of the RMP has been noticed in the developing mouse hindbrain (Kasper et al., 1994); in interneurons , (Ma et al., 2014) and for SS cells , (Valiullina et al., 2016). A larger age range may have been needed see this change, given that slight hyperpolarisation was found between the extremes of this dataset (P4 compared to P14). Typically, younger neurons have reported higher RMPs owing to high intracelullar Cl^- (Blaesse et al., 2009) which is caused by the late developmental insertion of a type of cotransport-protein, KCC2 (Chamma et al., 2012).

In similar discord with the literature, the membrane time constant did not appear to change with postnatal age. In experiments in prefrontal cortex pyramidal neurons, a long membrane time constant was found in immature slices, which shortened with age (Zhang, 2004). The proposed reasoning for this is that the long membrane time constant in immature allows for a greater capacity for temporal integration of synaptic responses. It seems likely that there would be shift in these membrane properties as the neuron develops its dendritic tree, establishes more connections, and has increased ion channel insertion.

The range of values seen in this report (62.6 – 31.5ms) is consistent with previous reports on SS cells when compared against the NeuroElectro database (Tripathy et al., 2014). It was hypothesised that τ_m would show a developmental decrease due to increases insertion of various ion channels, thereby increasing the speed by which SS neurons can respond to the current injection, however no significant decrease was detected. One argument for this is that decreasing R_i with development is linked to an overall increase in SS soma size as opposed to an increase in ion channels. However, given the dramatic changes seen in active dynamic properties (section 5.4) and previous reports studies into ion channel expression over the course of postnatal development (Moody and Bosma, 2005) this seems improbable . The increasing size of dendrites and cell size will have an impact on the cell's capacitance which in turn will be affecting the R_i and τ_m. While not directly measured in this investigation,

similar investigations have found an increase in capacitance over the first 2 weeks (Valiullina et al., 2016).

Nonetheless, the change seen here (with decreasing input resistance) and other studies (shortening membrane time constant; increased hyperpolarisation of RMP) with age, reflect that young neurons are more excitable, able to respond to weak input currents, and as they mature, rapidly transition to a more stable state. These observed changes could be as a result of increased K^+ transmission with postnatal age. Development-dependent alterations in K^+ currents have been noted in various neuronal subtypes, for example in hippocampal pyramidal cells (Fishell Rudy, 2011) interneurons (Tansey et al., 2002) and granule cells (Shibata et al., 2000). Overall, development of neural networks needs initial widespread activity of different populations of neurons, but as these networks develop, populations of neurons need to desynchronize activity to start the transformation from widespread circuit propagation to much more local and specific information processing (Khazipov and Luhmann, 2006; Yuste et al., 1995). Hence decreasing input resistance with age could be an inbuilt mechanism of reducing excitability. In general, an overall decrease in the range or variance of intrinsic properties in both R_i and RMP over P4-P14 could underlie the refinement of cortical networks.

5.3 How do active dynamics change with development?

It is clear that dramatic changes are seen in the AP waveform during the first 2 weeks: AP height increases by 80% and a AP width decreases by 83.7%, and sharp increases in their rising and falling phases with postnatal age. These changes are consistent with findings from investigations into barrel cortex postnatal development (Stern et al., 2001; Valiullina et al., 2016) and other cell types and brain regions (Annis et al., 1993; McCormick and Prince, 1987; Pan et al., 2016; Spigelman et al., 1992).

The developing AP should be looked at in the context of the changes happening to spiny stellate neurons as a whole over this time period, as the role of the AP may change with spiny stellate cell maturation. For example, spiny stellate cells fire APs prior to substantiate synapse formation and are thought to underlie synaptogenesis in early development (Spitzer et al., 2002). With postnatal development and the formation of synapses between stellate cells, APs have a role in mechanisms that select and eliminate specific connections – so-called 'synaptic pruning' which serves to eliminate the functionally obsolete, unspecific connections formed from an initial upsurge of synapses in very early development and preferentially strengthen functionally important connections (Katz and Shatz, 1996). In mature networks,

APs contribute to plasticity mechanisms and encode and transmit information rapidly; these processes are outlined in figure 5.1 below.

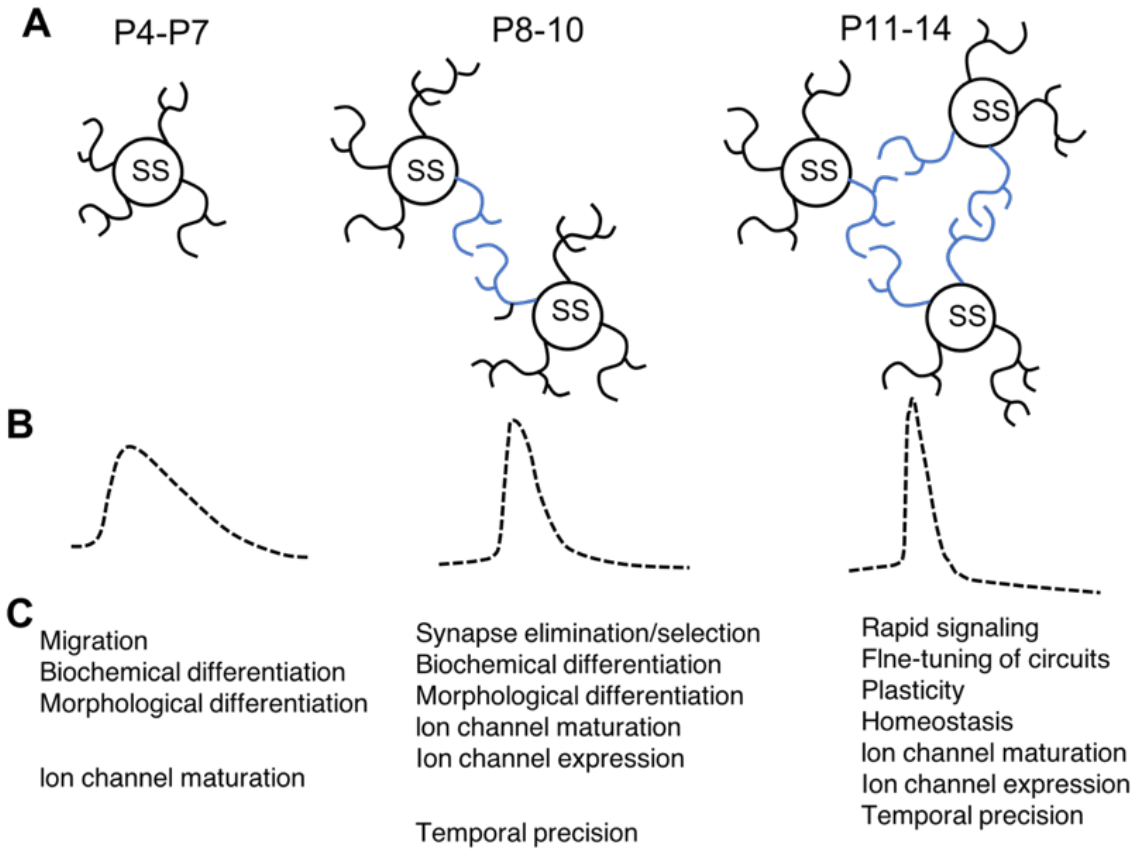

Fig. 5.1 **The role of SS neurons and APs change during postnatal development**
(A) schematic diagram of developing network of spiny stellate neurons across the set developmental age groups in this study, showing the increased dendritic branching and synaptic connections between SS cells with postnatal age (B) changes to the AP waveform in the first two weeks (C) descriptions of changes happening to spiny stellate neurons from early postnatal development to maturity, with dynamic changes in synapse elimination, and stabilisation.

Alterations to the expression and activation of ion channels are likely to underlie these development-dependent changes in AP waveform, though there is a lack of consensus about the exact pattern and temporality of these alterations. It is likely that the developing AP and its increase in rate of rise and fall (and subsequent effects on height and width) are underpinned by the developmental expression of potassium and sodium channels, which increase over the first two weeks (Moody & Bosma, 2005; Guan et al., 2011). Ion flux assays back up this argument, as they have revealed an increase in Na^+ (Huguenard et al., 1988) and K^+ (Costa et al., 1994; Spigelman et al., 1992b) conductance during development.

Increases in conductance are not just due to global increases in expression however, as shifts in channel subtype also underlie increased conductance; immunohistochemistry experiments by Kuba et al (2014) and RT-PCR experiments by (Van Wart and Matthews, 2006) have demonstrated a shift in sodium channel subtypes with postnatal development; specifically, a switch from Nav1.2 subtype dominance to Nav1.6 during the second postnatal week. These two subtypes have different voltage-dependent properties, with Nav1.2 displaying depolarised activation that allows for the conduction of APs at low frequencies, whereas Nav1.6 appears to support electrogenesis at higher frequencies (Rush et al., 2005), supporting the shift from immature to mature network formation.

In this investigation, maximum dV.dt became statistically different from P4 at P9 whereas minimum dV.dt became significantly different later in the developmental trajectory (P11). This indicates that the upstroke of the AP increases prior to an increase in min dV.dt; this makes sense when we consider that the min dV.dt corresponds to the part of the AP waveform associated with the closing of Na+ channels and opening of potassium channels, and perhaps indicates the order in which these events occur (i.e. the delayed significance of min dV.dt relative to the early dominance of max dV.dt could indicate that sodium channels are dominant and potassium channels have delayed opening).

A variety of potassium channels have been shown to be inserted during the first few days of life: in hippocampal neurons, several subtypes of a potassium channel family (Kv1) emerge in a set pattern, resulting in a sharp upsurge in the outward flow of potassium. These subunits also appear to be activity-dependent only during a set window of time, as blocking activation prevents their early function in postnatal development but does not results in downregulation in mature neurons (Moody and Bosma, 2005). In cortical interneurons, another potassium channel, Kv3, has been linked to AP-shortening with development: Golderberg et al (2011) found that AP width decreases in the first 2 weeks of life and that this change is concomitant with increased expression of Kv3.

It is likely that in-built ion channel regulation underpins AP development in spiny stellate cells, whereby the slow, short APs seen at P4-P7 in this study are due to low density levels of voltage-gated potassium channels with slow activation properties. The subsequent maturation of faster APs from P10 onwards seen in this study could therefore be due to a progressive increase in channel density and concomitant changes in channel activation kinetics. This would make sense if we consider that sodium channels develop ahead of potassium channels (Eijkelkamp et al., 2012). However, with an increase in Na^{+}-channels AP threshold did not appear to decrease over the first 2 weeks ($P>0.05$). This was surprising as previous reports on barrel cortex SS neurons (Vallulina et al., 2016) have commented on a small yet nonetheless significant negative change in threshold with maturation, reflecting the overall increase in

excitability of the circuit, although other studies have reported a lack of statistically significant changes in AP threshold over these time points (Vincent and Tell, 1997).

Certain intrinsic properties are likely to be related to increase in cell soma size (Callaway Borrell, 2011) and the upsurge in arborisation of neurites during P6-P9, where there is a notable increase in dendritic growth in spiny stellate cells (Espinosa et al., 2009; Mizuno et al., 2014), reflecting how the maturation of intrinsic properties is interrelated with the how synaptic inputs converge and change with postnatal age. The growing size of spiny stellate neurons and increasingly complex morphology will have impacts on the way SS cells generate APs. This morphological maturation, distinct from similar excitatory cells (e.g. pyramidal neurons, for example, go on to grow large apical dendrites), in part drives neuronal-specificity and could be important for initiating divergent downstream activity.

Changes in the morphology of the dendrite of SS cells will also have an impact on AP dynamics, as examined by electrophysiology experiments in the cortex on different neurons (Eyal et al., 2014; Hay et al., 2013) as well as computational models of how morphology influence AP dynamics (López-Jury et al., 2018). As the SS neurons grow in the first two weeks, and the larger their dendrites become, the more densely populated the axon initial segment (AIS) will be with excitable channels. Given this, one limitation to bear in mind is that in this investigation we have considered the axonal diameter to be fixed. It would therefore be useful to collect structural information about SS cells during this window of development to correlate electrophysiological data with SS cell size and shape.

The development of active dynamics is a crucial process for driving synapse formation and stabilisation in the cortex (Spitzer et al., 2002); and it is the combination of changing morphology and various active ion channel specialisations, shifts in function and expression which drive the maturation of temporally precise APs. The emergence of shorter and faster APs reflect the shift from immature circuits in the cortex being primed for spontaneous and evoked afferent activity to mature circuits, which are designed to encode and transmit information efficiently. The maturation in intrinsic properties is likely to underpin the way sensory information is relayed and disseminated in the somatosensory cortex, allowing for improved neuronal representation of sensory inputs.

5.4 Biocytin affects the intrinsic properties of spiny stellate cell

The internal solution is a crucial element of all electrophysiology investigations and increasingly the use of dyes in recording electrodes has been favoured to allow for reconstruction of

anatomical features of patched cells. However, several problems, not widely discussed in the literature, have been reported in the electrophysiological recordings of neurons patched with an intracellular label and then later used for morphological analysis. Protein labels or dyes can increase the resistance of the patching electrode, resulting in poor quality patches. The ideal dye should allow for a robust intracellular label that does not alter or in any way compromise the electrophysiological properties of the patched neuron. This investigation evaluated the use of three distinct internal solutions, one of which contained the dye biocytin, to see if the intrinsic properties of spiny stellate neurons were altered.

While some intrinsic parameters, were unaffected by internal solution, biocytin-patched cells showed significant differences in R_i and τ_m in older (P11-P14) SS neurons, but not at younger age-points. These effects were even more pronounced in the active dynamics of cells, with large differences seen in the kinetics of action potentials and in the shape of the AP waveform, with biocytin resulting in smaller APs of longer duration. Moreover, these effects remained when experiments were performed on SS neurons at higher (approximating physiological) temperatures, indicating that this finding was not due to an artefact in recording technique. The temperature-independent, age-dependent effects of Biocytin, particularly on spike waveform is a surprising finding, given that there is next to no discussion of this side-effect in the literature of dye-labelling in electrophysiology experiments.

Previous reports have commented on the effects of other dyes on intrinsic dynamics, such as HRP and Lucifer yellow (Stewart, 1981; Tasker et al., 1991) but biocytin is often heralded as the best marker for preserving intrinsic properties, with reports of negligible effects on the electrophysiological characteristics of recorded neurons (Horikawa & Armstrong, 1988; Tasker et al., 1991).

A dye very similar in composition to biocytin is neurobiotin (N-(2-aminoethyl)-biotinamide). Both biocytin and neurobiotin are hydrochloride salts (see figure); however, while the iso-electric point of biocytin is around 4.5-5.5 it (resulting in it carrying a small negative charge in neurtral pH), neurobiotin, by contrast has a much higher isoelectric point between 9.3-10.3 due to having no carboxylic acid attached (COOH; see figure) meaning it carries a overall positive charge in pH of around 7-8 (Kita and Armstrong, 1991).

Owing to its smaller size (M.W = 286, compared to M.W of 372, see figure above) neurobiotin has been reported to penetrate neurons coupled to patched cells via gap-junctions (Rörig et al., 1996; Swietek et al., 2016) and is often used for the detection of electrically coupled neurons. There is scant literature on the adverse effects of this dye on membrane properties, yet a few reports have found findings similar to those found in this report, such as increased spike-width (Schlösser et al., 1998; Xi and Xu, 1996) and decreased action potential height (Schlösser et al., 1998). Unpublished data suggests that neurobiotin in fact

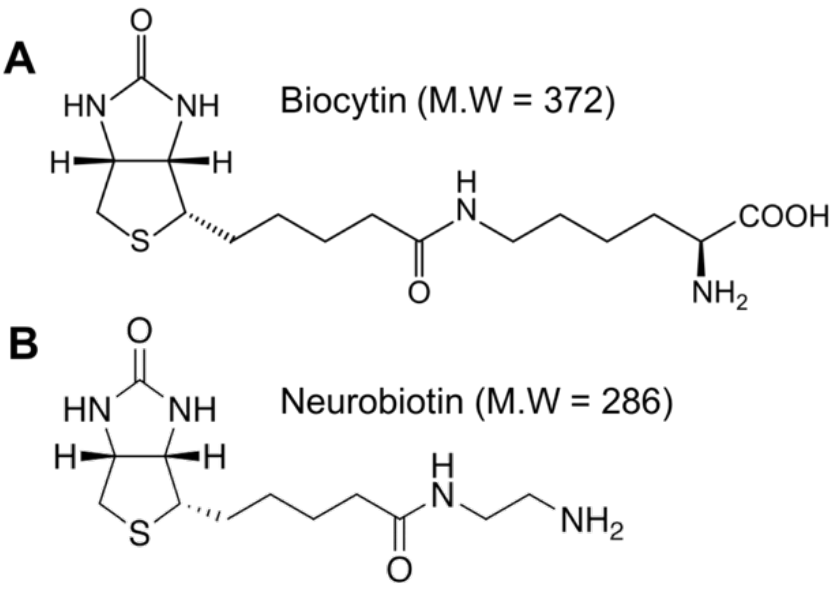

Fig. 5.2 **Chemical structures of biocytin (A) and neurobiotin (B).**

produces concentration-dependent effect on the active dynamics of the neurons, with similar findings of increased AP widths and reduced AP heights (Inkpen and Ashby; unpublished observation) which are significantly decreased at lower concentrations, indicating that there may be a 'safe' and 'unsafe' concertation of these dyes to use if post-hoc recovery is desired without alternation to intrinsic properties.

The experiments presented here indicate that in vitro whole cell electrophysiology using an internal solution containing biocytin, a compound regarded as biologically innocuous, can produce significant alterations the intrinsic properties of neurons. Effects of biocytin were observed at both room temperature and physiological temperature. An obvious conclusion (and word of caution) to these findings is that when using biocytin in electrophysiology experiments (e.g. for post-hoc staining) it is important not to ascribe aberrant effects to various treatments, age-models, or genotype comparison without comparing the effect of the compound biocytin alone. The data here indicate that spiny stellate neurons do not behave normally after being patched with biocytin-containing internal; though this must be regarded in the context of that is 'normal' for in vitro slice recordings vs in vivo states.

Across each of the 3 age categories and for each internal solution, no to the resting membrane potential occurred; this implies that biocytin that did not put SS cells in a compromised metabolic state, which would result in depolarisation of the RMP. One possibility is that biocytin is somehow damaging the plasma membrane of SS cells and causing 'leaky'

membranes, but given that it remains within neurons to allow for staining and there are no reported effects of this in the literature, this seems unlikely. The underlying basis for biocytin affecting both input resistance and membrane time constant at the later age range (P11-P14) is unknown. Equally, biocytin's effect of reducing the height and increasing the duration of AP waveforms is curious. However, the fact that the introduction of biocytin to the internal solution affects both the rate of rise and fall of APs suggests that biocytin might have multiple off-target channel effects that govern these changes. Most intuitively, it would seem that biocytin is affecting both sodium and potassium channels.

Future studies should address the mechanistic basis for the effects of biocytin on intrinsic properties, whether changes are also seen at an even earlier age point as to what has been reported here, and whether lower 'safer' concentrations cause the same effect.

5.5 Temperature's effects on intrinsic properties.

There was substantial temperature sensitivity of intrinsic membrane properties. Temperature had a noticeable impact on the active dynamics of the AP waveforms in slice-recordings, with increased thresholds, heights and widths at room temperatures. An increase in temperature corresponded to decreased R_i and τ_m, a finding consistent with literature for layer V pyramidal neurons (Waters, 2011), layer VI pyramidal neurons (Waters and Hedrick, 2012) neurons in the hippocampas (Thompson et al., 1985) and cortical neurons (Volgushev et al., 2000).

The changes seen in this study are likely a result of the sensitivity of VICs within the neuronal membranes. Lower temperatures affect VICs differently; while voltage-gated Na^+ channels have been reported to be unaffected by changes in temperature, potassium channels show high degrees of temperature sensitivity, with voltage-gated channels exhibiting higher activation thresholds (Volgushev et al., 2000) and an overall decrease in passive conductance of K^+. It has been suggested that lower temperatures also increase the electrical coupling between dendrites and cell bodies, which reflect reported changes in spiking dynamics, with lower temperatures yielding irregular spiking in pyramidal neurons (Waters and Hedrick, 2012; Waters, 2011). It proposed that the mechanism behind these changes is the disrupted ratio between potassium and sodium ions arising from the differential temperature sensitivities of their voltage-gated ion channels.

Temperature effects are widely considered in the literature by their individual 'temperature coefficient' or Q_{10}; this is the fold increase in rate with a 10-degree centrigrade increase (Fitzhugh, 1966). Many biological processes, such as ion channel movements described here, have a Q_{10}> 2 (Sterratt, 2015). Sodium channels are considered to have a Q_{10} of 2-4 (Egri and Ruben, 2012) while several potassium channels have a Q_{10} of around 20-30 (Yang and Zheng, 2014). This is relevant because potassium channels' wide ranging temperature sensitivity allows the voltage-gated channel to report changes in the membrane potential at different environmental states, allowing for reliable electrical signalling. Yet also, this altered ratio between K^+ and Na^+ conductances is what governs changes to the intrinsic properties of SS during heating or cooling; these changes to the intrinsic properties may lead to changes in synaptic transmission, with neurons potenitally being more excitable at lower temperatures (RT v PT).

While these results highlight the necessity of temperature-comparison of various intrinsic properties, they also demonstrate the confines of extrapolating conclusions from *in vitro* data to *in vivo* states given the stark change in intrinsic properties recorded at room temperature and physiological temperatures.

5.6 Limitations, future work and conclusions:

5.6.1 Future developments

A future development of this work would be to use imaging alongside electrophysiology so as to draw comparisons between the structural and functional development of cortical circuits. This addition is obvious given the use of biocytin in this study, as biocytin-labelling is a common method for visualizing cells in the cortex (Bender et al., 2003; Suter et al., 2013) and a development of this work could be to perform morphological reconstructions, as outlined by Bender et al., (2003) in their reconstruction of the topography of layer 4 axons in mouse somatosensory cortex. Equally, given the surprising finding of biocytin altering various intrinsic properties of cells, repeat experiments using lower concentrations of biocytin could be performed to determine an optimal concentration of dye without aberrant effects on electrophysiology. Investigating whether similar excitatory neurons (e.g. pyramidal neurons) and other classes of neuron (e.g. inhibitory interneurons neurons) have similar sensitivity to this compound at these concentrations would be of interest.

As all recordings in this project have been taken from a specific subtype of neuron (spiny stellate) in a specific region of the brain (barrel cortex) an obvious extension to the experiments presented here would be to compare the synaptic properties of SS cells by replicating the investigatiomns performed in this study in other cortical layers (layer 2/3, layer 5 or layer 6) and in alternative brain regions.

Such properties could then be compared in animal models of neurodevelopmental disorders. In this extension, several animal models are relevant: the original aim of this project was to perform genotype comparisons with a DISC1 mice as a model of schizophrenia, although due to difficulties importing the DISC1-cc mice from Cardiff – the transgenic mouse model originally created by Li et al., (2007) – this extension unfortunately did not go ahead. Nonetheless, this and several other animal models – such as the NRG1 (Stefansson et al., 2002) and DTNBP1 (Hattori et al., 2008) mouse models – present with identified neurodevelopmental alterations that result in irreversible cognitive deficits and other symptoms of schizophrenia in adult phenotypes. Given the somatosensory cortex's role in sensory processing and the identified changes in intrinsic properties in postnatal development in this study, comparing the neuronal dynamics of WT controls to these transgenic mouse models would be worthwhile.

The FMR1 knockout (FMR1-KO) mouse, a model of Fragile X Syndrome, would also be an interesting genotype comparison: FMR1-KO mice show distinctive alterations cognition (e.g. memory) and have been used to investigate CP plasticity in the barrel cortex (Domanski et al., 2018; Galvez and Greenough, 2005; Harlow et al., 2010; Till et al., 2012). Looking at

how the intrinsic properties of WT neurons develop postnatally and whether there are specific windows where alterations occur in neurodevelopmental disorders could provide insight into how aberrant network formation occurs, causing deficits like circuit hyperexcitability reported in adulthood. In the context of neurodevelopment it is curious that cognitive impairments occur in both schizophrenia and Fragile-X syndrome, but with differing onsets of impairment. In models of schizophirenia, such as DISC1, impairments occur in adolescence yet in Fragile-X models, such as the FMR1-KO, impairments are apparent early in postnatal development. In investigating the intrinsic properties and plasticity mechanisms underlying these transitions in development, we stand to gain a more nuanced understanding of how early postnatal development shapes adult brain functioning, potentially with great clinical impact. For example, could the cognitive problems associated with neurodevelopmental disorders be lessened if appropriate intervention took place at specific windows in postnatal maturation?

In a similar vein, it would be interesting to repeat these experiments with a sensory deprivation paradigm such as whisker trimming, to see how intrinsic properties are altered with sensory deprivation. This would be a useful comparison to see the importance of intrinsic properties on network formation, as perturbing sensory experience has been shown to have significant impacts upon network formation in early life (Ashby and Isaac, 2011; Cheetham et al., 2007; Fox, 1992; Lendvai et al., 2000).

As it is theorised that ion channel expression and insertion are critical to the development of active dynamic properties, looking at set changes in the pattern of VIC expression would be interesting. Analyses of these changes could be approached at the molecular level, such as identifying transcription factors for various VICs to ascertain whether these develop in set, coordinated trajectories, and whether alterations in these underlie various improper cortical circuit development. Building a developmental profile of ion channel expression could allow for greater awareness of the processes governing such biophysical changes in postnatal maturation.

5.6.2 Limitations

A limitation of this investigation is that chosen window of time (P4-P14) might obscure key developmental changes. Further measurements up to P21 would be beneficial for building a complete picture of intrinsic development, as this is when cortical circuit is considered to have reached maturity. Equally, more measurements at the other extreme of development would be useful, as starting at P4 could be missing key changes in early postnatal development.

One thing highlighted in this study is biophysical heterogeneity within the spiny stellate cell population – no two cells are exactly alike: even when one spiny stellate neuron was

patched and then its neighbouring cell was patched directly afterwards, there were distinct intrinsic properties specific to each cell, indicating the magnitude and ubiquity of cell to cell variation. The importance of recognising such within-type neuronal variation has been stressed elsewhere in the literature (Druckmann & Chklovskii, 2012; Padanahan & Urdan, 2010; Tripatty et al., 2014) when making comparisons between phenotypes. Comparison of this dataset to other literature is difficult due to subtle differences in experimental procedures, differences in species or strains of animals used, or differences in the age of animals used (there is a wealth of literature for spiny stellate neurons in mature animals, whereas studies on early postnatal ages similar to the range in this study are less common). If data is not consistent for a particular brain region in single mouse, a set of neuronal subtypes, or even a single subtype of cell, there must be progressively larger degrees of disparity when examining different cells, different regions, or different phenotypes. There are also limitations with drawing translational comparisons to human development with a mouse model of postnatal ageing, given the widespread differences in connectivity and neuroanatomy between mice and human brain tissue. Critically, a key limit to translation is that humans have a cortex that is 100x greater than that of mouse, do not have a 'barrel cortex' at all due to not having whiskers and there reported differences in the origins and developmetnal pathways for both neurons in primate cortex vs rodent cortex (Letinic et al., 2002). Such prominent distinctions between humans and rodents cause problems for equating the temporal and functional development of neurons directly.

5.6.3 Conclusion

In summary, the changes to the passive and active dynamics of spiny stellate neurons over the first two weeks of postnatal life are likely due to a combination of genetically pre-programmed changes to the VICs, and morphological changes in spiny stellate cells across the first 2 weeks. These changes also coincide with the transition from initial widespread activity to desynchronized activity patterns to allow for local and specific information processing. These changes in various intrinsic properties are interesting as they shed insight on the way these neurons integrate synaptic inputs and transmit information at different stages – and consideration of these temporally-specific alterations in SS neurons may be useful in animal models of neurodevelopmental disorders such as schizophrenia and fragile-X syndrome. The effects of both temperature and internal solution are important to consider when performing electrophysiology experiments, given the multifaceted impact these controls can have on neurophysiology.

Whilst further investigations are needed to unearth the processes underlying some of these changes seen in this study, these results highlight important biophysical changes that

occur in spiny stellate neurons in postnatal development to allow for functional networks in the adult cortex.